Leader-follower Formation Control with Prescribed Performance Guarantees

Fei Chen and Dimos V. Dimarogonas, *Senior Member, IEEE*

***Abstract*— This paper addresses the problem of achieving relative position-based formation control for leader-follower multi-agent systems in a distributed manner using a prescribed performance strategy. Both the first and second-order cases are treated and a leader-follower framework is introduced in the sense that a group of agents with external inputs are selected as leaders in order to drive the group of followers in a way that the entire system achieves a target formation within certain prescribed performance transient bounds. Under the assumption of tree graphs, a distributed control law is proposed for the first-order case when the decay rate of the performance functions is within a sufficient bound. Then, two classes of tree graphs that can have additional followers are investigated. For the second-order case, we propose a distributed control law based on a backstepping approach for the group of leaders to steer the entire system achieving the target formation within the prescribed performance bounds. Finally, several simulation examples are given to illustrate the results.**

***Index Terms*— Leader-follower control, formation control, multi-agent systems, prescribed performance control.**

I. Introduction

FORMATION control [1] of multi-agent systems has attracted great interest due to its wide applications in coordination of multiple robots. A formation is characterised as achieving or maintaining desired geometrical patterns via the cooperation of multiple agents. Relative position-based formation control methods are summarised in [2], where both the first and second-order relative position-based formation protocol are discussed. These are extended from the first and second-order consensus protocol, respectively. The first-order consensus protocol was first introduced in [3], while the second-order consensus protocol was investigated in [4].

In this work, we study relative position-based formation control in a leader-follower framework, that is, one or more agents are selected as *leaders* with external inputs in addition to the first or second-order formation protocol. The remaining agents are *followers* only obeying the first or second-order formation protocol. Recent research that has been done in the leader-follower framework can be divided into two parts. The first part deals with the controllability of leader-follower multi-agent systems. For instance, controllability of networked systems was first investigated in [5] by deriving conditions on the network topology, which ensures that the network can be controlled by a particular member which acts as a leader. The second part targets leader selection problems [6]–[8]. These involve the problem of how to choose the leaders among the agents such that the leader-follower system satisfies requirements such as controllability or optimal performance.

Prescribed performance control (PPC) was originally proposed in [9] to prescribe the evolution of system output or the tracking error within some predefined region. When it comes to multi-agent systems, an agreement protocol that can additionally achieve prescribed performance for a combined error of positions and velocities was designed in [10] for multi-agent systems with double integrator dynamics, while PPC for multi-agent average consensus with single integrator dynamics was presented in [11]. Funnel control, which uses a similar idea as PPC was first introduced in [12] for reference tracking.

In this work, both first and second-order leader-follower multi-agent systems are treated and we are interested in how to design control strategies for the leaders such that the leader-follower multi-agent system achieves a relative position-based formation within certain performance bounds. Compared with existing work of PPC for multi-agent systems [10], we apply a PPC law only to the leaders while most of the related work, including [10], applies PPC to all the agents to achieve here tasks such as consensus or formation. The benefit of this work is to lower the cost of the control effort since the followers will follow the leaders by obeying first or second-order formation protocols without any additional control and knowledge of the prescribed team bounds. Unlike other approaches for leader-follower multi-agent systems using PPC [13], in which the multi-agent system only has one leader and the leader is treated as a reference for the followers, we focus on a more general framework in the sense that we can have more than one leader and the leaders are designed in order to steer the entire system achieving the target formation within the prescribed performance bounds. The difficulties in this work are due to the combination of uncertain topologies, leader amount and leader positions. In addition, the leader can only communicate with its neighbouring agents. The contributions of the paper can be summarized as: i) within this general leader-follower framework, under the assumption of tree graphs, a distributed control law is proposed when the decay rate of the performance functions is within a sufficient bound; ii) the specific classes of chain and star graphs that can have additional followers are investigated; iii) for second-order case,

This work was supported by the ERC Consolidator Grant LEAFHOUND, the EU H2020 Co4Robots Project, the Swedish Research Council (VR) and the Knut och Alice Wallenberg Foundation (KAW).

Fei Chen and Dimos V. Dimarogonas are with the Division of Decision and Control Systems, KTH Royal Institute of Technology, SE-100 44 Stockholm, Sweden {fchen, dimos}@kth.se.

we propose a distributed control law based on a backstepping approach for the group of leaders to steer the entire system to a target formation within certain prescribed performance transient bounds for the whole team. Preliminary results of first and second-order consensus for leader-follower multi-agent systems with prescribed performance guarantees have been presented in [14], [15], respectively. In this work, we extend our previous results to the relative position-based formation. In particular, under the leader-follower framework, PPC is utilized in order to achieve the target formation along with the prescribed performance guarantees. Applying PPC to formation control has more practical applications when compared to applying PPC to consensus. For example, in cooperative formation control, a key topic is collision avoidance and connectivity maintenance, which can be tackled by prescribed performance control. Thus this first result of leader-follower formation control using PPC offers a more general framework and paves the way for more general structures of the formation than consensus. The challenges of uncertain leader-follower topology also exist when considering formation control in the leader-follower framework. Finally, several two-dimensional simulations showing the target relative position-based formations are added in order to verify the results.

The rest of the paper is organized as follows. In Section II, preliminary knowledge is introduced and the problem is formulated, while Section III presents the main results, where both the first and second-order cases are discussed. The results are further verified by simulation examples in Section IV. Section V includes conclusions and future work.

II. PRELIMINARIES AND PROBLEM STATEMENT

A. Graph Theory

An undirected graph [16] is defined as $\mathcal{G} = (\mathcal{V}, \mathcal{E})$ with the vertices set $\mathcal{V} = \{1, 2, \ldots, n\}$ and the edges set $\mathcal{E} = \{(i, j) \in \mathcal{V} \times \mathcal{V} \mid j \in \mathcal{N}_i\}$ indexed by $e_1, \ldots, e_m$. Here, $m = |\mathcal{E}|$ is the number of edges and $\mathcal{N}_i$ denotes the neighbourhood of agent i such that agent $j \in \mathcal{N}_i$ can communicate with i. A *path* is a sequence of edges connecting two distinct vertices. A graph is *connected* if there exists a path between any pair of vertices. By assigning an orientation to each edge of $\mathcal{G}$ the *incidence matrix* $D = D(\mathcal{G}) = [d_{ij}] \in \mathbb{R}^{n\times m}$ is defined. The rows of D are indexed by the vertices and the columns are indexed by the edges with $d_{ij} = 1$ if the vertex i is the head of the edge (i, j), $d_{ij} = -1$ if the vertex i is the tail of the edge (i, j) and $d_{ij} = 0$ otherwise. The *graph Laplacian* of $\mathcal{G}$ is described as $L = DD^T$. In addition, $L_e = D^T D$ is the so called *edge Laplacian* [17] and $(L_e)_{ij} = c_{ij}$ denotes the elemnts of L_e.

B. System Description

In this work, we consider a multi-agent system with vertices $\mathcal{V} = \{1, 2, \ldots, n\}$. Without loss of generality, we suppose that the first n_f agents are selected as followers while the last n_l agents are selected as leaders with respective vertices set $\mathcal{V}_F = \{1, \ldots, n_f\}$, $\mathcal{V}_L = \{n_f + 1, \ldots, n_f + n_l\}$ and $n = n_f + n_l$.

Let $p_i, v_i \in \mathbb{R}$ be the respective position and velocity of agent i, where we only consider the one dimensional case, without loss of generality. Specifically, the results can be extended to higher dimensions with appropriate use of the Kronecker product. This work aims to design a control strategy for the leader-follower multi-agent system such that it can achieve the following target relative position-based formation

$$\mathcal{F} := \{p \mid p_i - p_j = p_{ij}^{des}, (i, j) \in \mathcal{E}\}, \tag{1}$$

where $p_{ij}^{des} := p_i^{des} - p_j^{des}, (i, j) \in \mathcal{E}$ is the desired relative position between agent i and agent j, which is constant and denoted as the difference between the absolute desired spositions $p_i^{des}, p_j^{des} \in \mathbb{R}$. Here, p_{ij}^{des} is only needed to be known and p_i^{des}, p_j^{des} are defined with respect to an arbitrary reference frame and do not need to be known.

In the first-order case, the state evolution of each follower $i \in \mathcal{V}_F$ is governed by the first-order formation protocol:

$$\dot{p}_i = -\sum_{j\in\mathcal{N}_i} (p_i - p_j - p_{ij}^{des}). \tag{2}$$

The state evolution of each leader $i \in \mathcal{V}_L$ is governed by the first-order formation protocol with an external input $u_i \in \mathbb{R}$:

$$\dot{p}_i = -\sum_{j\in\mathcal{N}_i} (p_i - p_j - p_{ij}^{des}) + u_i. \tag{3}$$

In the second-order case, the state evolution of each follower $i \in \mathcal{V}_F$ is governed by the second-order formation protocol:

$$\begin{aligned} \dot{p}_i &= v_i \\ \dot{v}_i &= -\sum_{j\in\mathcal{N}_i} \left((p_i - p_j - p_{ij}^{des}) + (v_i - v_j)\right). \end{aligned} \tag{4}$$

The state evolution of leader $i \in \mathcal{V}_L$ is governed by the second-order formation protocol with an external input $u_i \in \mathbb{R}$:

$$\begin{aligned} \dot{p}_i &= v_i \\ \dot{v}_i &= -\sum_{j\in\mathcal{N}_i} \left((p_i - p_j - p_{ij}^{des}) + (v_i - v_j)\right) + u_i. \end{aligned} \tag{5}$$

Let us denote $p = [p_1, \ldots, p_n]^T, v = [v_1, \ldots, v_n]^T, p^{des} = [p_1^{des}, \ldots, p_n^{des}]^T \in \mathbb{R}^n$ as the respective stack vector of absolute positions, velocities and target positions and $u = [u_{n_f+1}, \ldots, u_{n_f+n_l}]^T \in \mathbb{R}^{n_l}$ is the control input vector including the external inputs of leader agents in (3), (5). Denote $\bar{p} = [\bar{p}_1, \ldots, \bar{p}_m]^T$, $\bar{v} = [\bar{v}_1, \ldots, \bar{v}_m]^T, \bar{p}^{des} = [\bar{p}_1^{des}, \ldots, \bar{p}_m^{des}]^T \in \mathbb{R}^m$ as the respective stack vector of relative positions, relative velocities and target relative positions between the pair of communication agents for the edge $(i, j) = k \in \mathcal{E}$, where $\bar{p}_k \triangleq p_{ij} = p_i - p_j, \bar{v}_k \triangleq v_{ij} = v_i - v_j, \bar{p}_k^{des} \triangleq p_{ij}^{des} = p_i^{des} - p_j^{des}, k = 1, 2, \ldots, m$. It can be then verified that $Lp = D\bar{p}$ and $\bar{p} = D^T p$. In addition, if $\bar{p} = 0$, we have that $Lp = 0$. Similarly, it holds that $Lv = D\bar{v}$, $\bar{v} = D^T v$ and $Lp^{des} = D\bar{p}^{des}$, $\bar{p}^{des} = D^T p^{des}$.

By stacking (2), (3), the dynamics of the first-order leader-follower multi-agent system is rewritten as:

$$\Sigma_1 : \dot{p} = -L(p - p^{des}) + Bu. \tag{6}$$

Similarly, stacking (4) and (5), the dynamics of the second-order leader-follower multi-agent system is rewritten as:

$$\Sigma_2 : \begin{bmatrix} \dot{p} \\ \dot{v} \end{bmatrix} = \begin{bmatrix} 0_n & I_n \\ -L & -L \end{bmatrix} \begin{bmatrix} p - p^{des} \\ v \end{bmatrix} + \begin{bmatrix} 0_{n\times n_l} \\ B \end{bmatrix} u, \tag{7}$$

where L is the graph Laplacian and $B = \begin{bmatrix} 0_{n_f \times n_l} \\ I_{n_l} \end{bmatrix}$.

In the sequel, we denote $x = p - p^{des} = [x_1, \ldots, x_n]^T$ as the shifted absolute position vector with respect to p^{des}. Accordingly, $\bar{x} = \bar{p} - \bar{p}^{des} = [\bar{x}_1, \ldots, \bar{x}_m]^T$ is denoted as the shifted relative position vector with respect to $\bar{p}^{des}$.

C. Prescribed Performance Control

The aim of PPC is to prescribe the evolution of the relative position $\bar{p}_i(t)$ within some predefined region described as

$$\bar{p}_i^{des} - \rho_{\bar{x}_i}(t) < \bar{p}_i(t) < \bar{p}_i^{des} + \rho_{\bar{x}_i}(t), \tag{8}$$

or equivalently, to prescribe the evolution of the shifted relative position $\bar{x}_i(t)$ within

$$-\rho_{\bar{x}_i}(t) < \bar{x}_i(t) < \rho_{\bar{x}_i}(t). \tag{9}$$

(8) and (9) are equivalent since $\bar{x} = \bar{p} - \bar{p}^{des}$ (while in component format also). Here $\rho_{\bar{x}_i}(t) : \mathbb{R}_+ \to \mathbb{R}_+ \setminus \{0\}, i = 1, 2, \ldots, m$ are positive, smooth and strictly decreasing performance functions that introduce the predefined bounds for the shifted relative positions. One example choice is

$$\rho_{\bar{x}_i}(t) = (\rho_{\bar{x}_{i0}} - \rho_{\bar{x}_{i\infty}})e^{-l_{\bar{x}_i} t} + \rho_{\bar{x}_{i\infty}}. \tag{10}$$

with $\rho_{\bar{x}_{i0}}, \rho_{\bar{x}_{i\infty}}$ and $l_{\bar{x}_i}$ positive parameters and $\rho_{\bar{x}_{i\infty}} = \lim_{t\to\infty} \rho_{\bar{x}_i}(t)$ represents the maximum allowable tracking error at steady state.

Normalizing $\bar{x}_i(t)$ with respect to the performance function $\rho_{\bar{x}_i}(t)$, we define the modulated error as $\hat{\bar{x}}_i(t)$ and the corresponding prescribed performance region $\mathcal{D}_{\bar{x}_i}$ as:

$$\hat{\bar{x}}_i(t) = \frac{\bar{x}_i(t)}{\rho_{\bar{x}_i}(t)}, \tag{11}$$

$$\mathcal{D}_{\bar{x}_i} \triangleq \{\hat{\bar{x}}_i : \hat{\bar{x}}_i \in (-1, 1)\}. \tag{12}$$

Then the modulated error is transformed through a transformed function $T_{\bar{x}_i}$ that defines the smooth and strictly increasing mapping $T_{\bar{x}_i} : \mathcal{D}_{\bar{x}_i} \to \mathbb{R}$, $T_{\bar{x}_i}(0) = 0$. One example choice is

$$T_{\bar{x}_i}(\hat{\bar{x}}_i) = \ln\left(\frac{1 + \hat{\bar{x}}_i}{1 - \hat{\bar{x}}_i}\right). \tag{13}$$

The transformed error is then defined as

$$\varepsilon_{\bar{x}_i}(\hat{\bar{x}}_i) = T_{\bar{x}_i}(\hat{\bar{x}}_i) \tag{14}$$

It can be verified that if the transformed error $\varepsilon_{\bar{x}_i}(\hat{\bar{x}}_i)$ is bounded, then the modulated error $\hat{\bar{x}}_i$ is constrained within the region (12). This also implies the error $\bar{x}_i$ evolves within the predefined performance bounds (9). Differentiating (14) with respect to time, we derive

$$\dot{\varepsilon}_{\bar{x}_i}(\hat{\bar{x}}_i) = \mathcal{J}_{T_{\bar{x}_i}}(\hat{\bar{x}}_i, t)[\dot{\bar{x}}_i + \alpha_{\bar{x}_i}(t)\bar{x}_i] \tag{15}$$

where

$$\mathcal{J}_{T_{\bar{x}_i}}(\hat{\bar{x}}_i, t) \triangleq \frac{\partial T_{\bar{x}_i}(\hat{\bar{x}}_i)}{\partial \hat{\bar{x}}_i} \frac{1}{\rho_{\bar{x}_i}(t)} > 0 \tag{16}$$

$$\alpha_{\bar{x}_i}(t) \triangleq -\frac{\dot{\rho}_{\bar{x}_i}(t)}{\rho_{\bar{x}_i}(t)} > 0 \tag{17}$$

are the normalized Jacobian of the transformed function $T_{\bar{x}_i}$ and the normalized derivative of the performance function, respectively.

D. Problem Statement

In this work, we aim to design a control strategy for the leader-follower multi-agent system (6) or (7) such that it can achieve the target formation $\mathcal{F}$ as in (1). In addition, the control strategy is only applied to the leaders and the evolution of the relative positions between neighbouring agents should satisfy the prescribed performance bounds (8). Formally,

Problem 1: Let the leader-follower multi-agent system Σ be defined by (6) or (7) with the communication graph $\mathcal{G} = (\mathcal{V}, \mathcal{E})$ and the prescribed performance functions $\rho_{\bar{x}_i}, i = 1, 2, \ldots, m$. Derive a ladder control strategy such that the controlled leader-follower multi-agent system achieves the target formation $\mathcal{F}$ as in (1) while satisfying (8).

III. MAIN RESULTS

In this section, we design the control for the leader-follower multi-agent system (6) and (7) such that the system can achieve the target formation $\mathcal{F}$ as in (1) within the prescribed performance bounds (8). The respective performance functions $\rho_{\bar{x}_i}(t)$ and transformed functions $T_{\bar{x}_i}(\hat{\bar{x}}_i)$ are defined as (10) and (13) without loss of generality. The later results can be generalised to any positive, smooth and strictly decreasing functions $\rho_{\bar{x}_i}(t)$, and any smooth and strictly increasing transformed functions $T_{\bar{x}_i} : \mathcal{D}_{\bar{x}_i} \to \mathbb{R}$ that go through the origin. We assume that communicating agents share information about their performance functions $\rho_{\bar{x}_i}(t)$ and transformed functions $T_{\bar{x}_i}(\hat{\bar{x}}_i)$. Hence, the communication between neighbouring agents is bidirectional and the graph $\mathcal{G}$ is assumed undirected.

A. Formation control of first-order case using PPC

Since our target is the relative position-based formation and the prescribed performance functions are defined based on $\bar{x}$, we first rewrite the dynamics of the leader-follower multi-agent system (6) into the edge space in order to characterise the dynamics of the relative positions. We then rewrite (6) into the dynamics corresponding to followers and leaders, respectively. The corresponding incidence matrix is decomposed into the first n_f and the remaining last n_l rows, i.e., $D = \begin{bmatrix} D_F^T & D_L^T \end{bmatrix}^T$ [16] with D_F, D_L denoting the incidence matrices with respect to the followers and leaders, respectively. Using $x = p - p^{des}$, the dynamics (6) are reorganised as

$$\Sigma_1 : \begin{bmatrix} \dot{x}_F \\ \dot{x}_L \end{bmatrix} = \begin{bmatrix} A_F & B_F \\ B_F^T & A_L \end{bmatrix} \begin{bmatrix} x_F \\ x_L \end{bmatrix} + \begin{bmatrix} 0_{n_f \times n_l} \\ I_{n_l} \end{bmatrix} u, \tag{18}$$

where $x_F = [x_1, \ldots, x_{n_f}]^T, x_L = [x_{n_f+1}, \ldots, x_n]^T$ and $A_F = D_F D_F^T, B_F = D_F D_L^T, A_L = D_L D_L^T$. Multiplying with D^T on both sides of (18), we obtain the dynamics on the edge space as

$$\Sigma_{e1} : \dot{\bar{x}} = -L_e \bar{x} + D_L^T u, \tag{19}$$

with L_e as the edge Laplacian and L_e is positive definite if the graph is a tree [18]. We thus here assume the following.

Assumption 1: The graph $\mathcal{G} = (\mathcal{V}, \mathcal{E})$ is a tree.

We consider tree graphs as a starting point since we need the positive definiteness of L_e in the analysis, and motivated by the fact that they require less communication load (less edges) for their implementation. Note however that further results for a general graph could be built based on the results of tree graphs, e.g., through graph decompositions [17]. For the edge dynamics (19), the proposed controller applied to the leader agents is the composition of the term based on prescribed performance of the positions of the neighbouring agents:

$$u_j = -\sum_{i\in\Phi_j} g_{\bar{x}_i}\mathcal{J}_{T_{\bar{x}_i}}(\hat{\bar{x}}_i,t)\varepsilon_{\bar{x}_i}(\hat{\bar{x}}_i), \qquad j\in\mathcal{V}_L, \tag{20}$$

where $\Phi_j = \{i|(j,k)=i, k\in\mathcal{N}_j\}$, i.e., the set of all the edges that include agent $j\in\mathcal{V}_L$ as a node, and $g_{\bar{x}_i}$ is a positive scalar gain to be appropriately tuned. Then the stack input vector is

$$u = -D_L\mathcal{J}_{T_{\hat{\bar{x}}}}G_{\bar{x}}\varepsilon_{\hat{\bar{x}}}, \tag{21}$$

where $\hat{\bar{x}}\in\mathbb{R}^m$ is the stack vector of transformed errors $\hat{\bar{x}}_i$, $G_{\bar{x}}\in\mathbb{R}^{m\times m}$ is the positive definite diagonal gain matrix with entries the positive constant parameters $g_{\bar{x}_i}$, $\mathcal{J}_{T_{\hat{\bar{x}}}} \triangleq \mathcal{J}_T(\hat{\bar{x}},t)\in\mathbb{R}^{m\times m}$ is a time varying diagonal matrix with diagonal entries $\mathcal{J}_{T_{\bar{x}_i}}(\hat{\bar{x}}_i,t)$ given in (16), and $\varepsilon_{\hat{\bar{x}}}\triangleq\varepsilon(\hat{\bar{x}})\in\mathbb{R}^m$ is the stack vector with entries $\varepsilon_{\bar{x}_i}(\hat{\bar{x}}_i)$. Then the edge dynamics (19) with input (21) can be written as

$$\dot{\bar{x}} = -L_e\bar{x} - D_L^TD_L\mathcal{J}_{T_{\hat{\bar{x}}}}G_{\bar{x}}\varepsilon_{\hat{\bar{x}}}, \tag{22}$$

In the sequel, we develop the following result and will use Lyapunov-like methods to prove that the target formation can be achieved and the prescribed performance can be guaranteed.

Theorem 1: Consider the leader-follower multi-agent system Σ_1 under Assumption 1 with dynamics (6), the predefined performance functions $\rho_{\bar{x}_i}$ as in (10) and the transformed functions $T_{\bar{x}_i}(\hat{\bar{x}}_i)$ as in (13) s.t. $T_{\bar{x}_i}(0)=0$, and assume that the initial conditions $\bar{p}_i(0)$ are within the performance bounds (8). If the following condition holds:

$$\bar{\gamma}\geq l = \max_{i=1,\dots,m}(l_{\bar{x}_i}), \tag{23}$$

where l is the largest decay rate of $\rho_{\bar{x}_i}(t)$ and $\bar{\gamma}$ is the maximum value of γ that ensures:

$$\Gamma = \begin{bmatrix} D_L^TD_L & \frac{1}{2}\big(L_e-\gamma\big(I_m-D_L^TD_L\big)\big) \\ \frac{1}{2}\big(L_e-\gamma\big(I_m-D_L^TD_L\big)\big) & \gamma L_e\end{bmatrix}\geq 0, \tag{24}$$

then the controlled system achieves the target formation (1) and satisfies (8) when applying the control law (21).

Proof: The underlying idea of the proof is based on showing that $\varepsilon_{\hat{\bar{x}}}$ is bounded through a candidate Lyapunov function. Then, the boundedness of $\varepsilon_{\hat{\bar{x}}}$ implies that the modulated error $\hat{\bar{x}}_i$ is constrained within the region (12). This further implies that the error $\bar{x}_i$ evolves within the predefined performance bounds (9). Since the initial conditions $\bar{p}_i(0)$ are within the performance bounds (8), this is equivalent to that the initial conditions $\bar{x}_i(0)$ are within the performance bounds (9). Consider the Lyapunov-like function

$$V(\varepsilon_{\hat{\bar{x}}},\bar{x}) = \frac{1}{2}\varepsilon_{\hat{\bar{x}}}^TG_{\bar{x}}\varepsilon_{\hat{\bar{x}}} + \frac{\gamma}{2}\bar{x}^T\bar{x}. \tag{25}$$

Then, $\dot{V} = \varepsilon_{\hat{\bar{x}}}^TG_{\bar{x}}\dot{\varepsilon}_{\hat{\bar{x}}} + \gamma\bar{x}^T\dot{\bar{x}}$. Replacing $\dot{\varepsilon}_{\hat{\bar{x}}}$ by stacking the components $\dot{\varepsilon}_{\bar{x}_i}(\hat{\bar{x}}_i)$ that are derived in (15), we obtain $\dot{V} = \varepsilon_{\hat{\bar{x}}}^TG_{\bar{x}}\mathcal{J}_{T_{\hat{\bar{x}}}}(\dot{\bar{x}}+\alpha_{\bar{x}}(t)\bar{x}) + \gamma\bar{x}^T\dot{\bar{x}}$, where $\alpha_{\bar{x}}(t)$ is the diagonal matrix with diagonal entries $\alpha_{\bar{x}_i}(t)$. According to (17) and (10), we know that

$$\alpha_{\bar{x}_i}(t)\triangleq -\frac{\dot{\rho}_{\bar{x}_i}(t)}{\rho_{\bar{x}_i}(t)} = l_{\bar{x}_i}\frac{\rho_{\bar{x}_i}(t)-\rho_{\bar{x}_{i\infty}}}{\rho_{\bar{x}_i}(t)} < l_{\bar{x}_i}, \forall t. \tag{26}$$

Substituting (22), we can further derive that

$$\begin{aligned}\dot{V} =& \varepsilon_{\hat{\bar{x}}}^TG_{\bar{x}}\mathcal{J}_{T_{\hat{\bar{x}}}}(-L_e\bar{x} - D_L^TD_L\mathcal{J}_{T_{\hat{\bar{x}}}}G_{\bar{x}}\varepsilon_{\hat{\bar{x}}} + \alpha_{\bar{x}}(t)\bar{x}) \\ &+ \gamma\bar{x}^T(-L_e\bar{x} - D_L^TD_L\mathcal{J}_{T_{\hat{\bar{x}}}}G_{\bar{x}}\varepsilon_{\hat{\bar{x}}}) \\ =& -\varepsilon_{\hat{\bar{x}}}^TG_{\bar{x}}\mathcal{J}_{T_{\hat{\bar{x}}}}L_e\bar{x} + \varepsilon_{\hat{\bar{x}}}^TG_{\bar{x}}\mathcal{J}_{T_{\hat{\bar{x}}}}\alpha_{\bar{x}}(t)\bar{x} \\ &- \varepsilon_{\hat{\bar{x}}}^TG_{\bar{x}}\mathcal{J}_{T_{\hat{\bar{x}}}}D_L^TD_L\mathcal{J}_{T_{\hat{\bar{x}}}}G_{\bar{x}}\varepsilon_{\hat{\bar{x}}} - \gamma\bar{x}^TL_e\bar{x} \\ &- \gamma\bar{x}^TD_L^TD_L\mathcal{J}_{T_{\hat{\bar{x}}}}G_{\bar{x}}\varepsilon_{\hat{\bar{x}}}\end{aligned} \tag{27}$$

Adding and subtracting $\gamma\varepsilon_{\hat{\bar{x}}}^TG_{\bar{x}}\mathcal{J}_{T_{\hat{\bar{x}}}}\bar{x}$ on the right hand side of (27), we obtain

$$\begin{aligned}\dot{V} =& -\varepsilon_{\hat{\bar{x}}}^TG_{\bar{x}}\mathcal{J}_{T_{\hat{\bar{x}}}}(\gamma I_m - \alpha_{\bar{x}}(t))\bar{x} \\ &- \varepsilon_{\hat{\bar{x}}}^TG_{\bar{x}}\mathcal{J}_{T_{\hat{\bar{x}}}}D_L^TD_L\mathcal{J}_{T_{\hat{\bar{x}}}}G_{\bar{x}}\varepsilon_{\hat{\bar{x}}} \\ &- \varepsilon_{\hat{\bar{x}}}^TG_{\bar{x}}\mathcal{J}_{T_{\hat{\bar{x}}}}L_e\bar{x} - \gamma\bar{x}^TL_e\bar{x} \\ &+ \gamma\varepsilon_{\hat{\bar{x}}}^TG_{\bar{x}}\mathcal{J}_{T_{\hat{\bar{x}}}}(I_m - D_L^TD_L)\bar{x} \\ =& -\varepsilon_{\hat{\bar{x}}}^TG_{\bar{x}}\mathcal{J}_{T_{\hat{\bar{x}}}}(\gamma I_m - \alpha_{\bar{x}}(t))\bar{x} \\ &- y^T\begin{bmatrix} D_L^TD_L & \frac{1}{2}\big(L_e-\gamma\big(I_m-D_L^TD_L\big)\big) \\ \frac{1}{2}\big(L_e-\gamma\big(I_m-D_L^TD_L\big)\big) & \gamma L_e\end{bmatrix}y \\ =& -\varepsilon_{\hat{\bar{x}}}^TG_{\bar{x}}\mathcal{J}_{T_{\hat{\bar{x}}}}(\gamma I_m - \alpha_{\bar{x}}(t))\bar{x} - y^T\Gamma y\end{aligned} \tag{28}$$

with $y = \begin{bmatrix}\varepsilon_{\hat{\bar{x}}}^TG_{\bar{x}}\mathcal{J}_{T_{\hat{\bar{x}}}} & \bar{x}^T\end{bmatrix}^T$. Since $G_{\bar{x}}, \mathcal{J}_{T_{\hat{\bar{x}}}}$ are both diagonal and positive definite matrices, we have that $G_{\bar{x}}\mathcal{J}_{T_{\hat{\bar{x}}}}$ is also a diagonal positive definite matrix; $(\gamma I_m - \alpha_{\bar{x}}(t))$ is a diagonal positive definite matrix if $\gamma\geq l = \max(l_{\bar{x}_i}) > \bar{\alpha} = \sup\alpha_{\bar{x}_i}(t)$. Since the transformed function $T_{\bar{x}_i}(\hat{\bar{x}}_i)$ is strictly increasing and $T_{\bar{x}_i}(0)=0$, we have $\varepsilon_{\bar{x}_i}(\hat{\bar{x}}_i)\hat{\bar{x}}_i = T_{\bar{x}_i}(\hat{\bar{x}}_i)\hat{\bar{x}}_i\geq 0$. Then, by setting $\gamma := \theta+\bar{\alpha}$, with θ being a positive constant we get that $-\varepsilon_{\hat{\bar{x}}}^TG_{\bar{x}}\mathcal{J}_{T_{\hat{\bar{x}}}}(\gamma I_m - \alpha_{\bar{x}}(t))\bar{x}\leq -\theta\varepsilon_{\hat{\bar{x}}}^TG_{\bar{x}}\mathcal{J}_{T_{\hat{\bar{x}}}}\bar{x}$ Then, according to (11), (14), (16), we have that $\mathcal{J}_{T_{\bar{x}_i}}(\hat{\bar{x}}_i,t)\bar{x}_i = \frac{\partial T_{\bar{x}_i}(\hat{\bar{x}}_i)}{\partial\hat{\bar{x}}_i}\frac{1}{\rho_{\bar{x}_i}(t)}\rho_{\bar{x}_i}(t)\hat{\bar{x}}_i = \frac{\partial\varepsilon_{\bar{x}_i}(\hat{\bar{x}}_i)}{\partial\hat{\bar{x}}_i}\hat{\bar{x}}_i$. We thus further obtain

$$-\theta\varepsilon_{\hat{\bar{x}}}^TG_{\bar{x}}\mathcal{J}_{T_{\hat{\bar{x}}}}\bar{x} = -\theta\varepsilon_{\hat{\bar{x}}}^TG_{\bar{x}}\frac{\partial\varepsilon_{\hat{\bar{x}}}}{\partial\hat{\bar{x}}}\hat{\bar{x}}\leq 0. \tag{29}$$

(29) holds because the transformed function is smooth and strictly increasing and $\varepsilon_{\bar{x}_i}(\hat{\bar{x}}_i)\hat{\bar{x}}_i\geq 0$. Therefore, in order for $\dot{V}\leq 0$ to hold, it suffices that $\gamma\geq l = \max(l_{\bar{x}_i}) > \sup\alpha_{\bar{x}_i}(t)$ and in addition, Γ should be semi-positive definite. Then, based on condition (23), and choosing $\gamma=\bar{\gamma}$, we obtain $-\varepsilon_{\hat{\bar{x}}}^TG_{\bar{x}}\mathcal{J}_{T_{\hat{\bar{x}}}}(\bar{\gamma}I_m - \alpha_{\bar{x}}(t))\bar{x}\leq 0$ and $\Gamma\geq 0$. Finally, we can conclude that $\dot{V}\leq 0$ when $\gamma=\bar{\gamma}$. This also implies $V(\varepsilon_{\hat{\bar{x}}},\bar{x})\leq V(\varepsilon_{\hat{\bar{x}}}(0),\bar{x}(0))$. Hence if $\bar{x}(0))$ is chosen within the region (12) then $V(\varepsilon_{\hat{\bar{x}}}(0),\bar{x}(0))$ is finite, which implies that $V(\varepsilon_{\hat{\bar{x}}},\bar{x})$ is bounded $\forall t$. Therefore $\varepsilon_{\hat{\bar{x}}},\bar{x}$ are bounded and the boundedness of the transformed error $\varepsilon_{\hat{\bar{x}}}$ implies that the relative position $\bar{x}(t)$ evolves within the prescribed performance bounds (9), $\forall t$. Then we can deduce the boundedness of $\ddot{V}(\varepsilon_{\hat{\bar{x}}},\bar{x})$ based on the boundedness of $\varepsilon_{\hat{\bar{x}}},\dot{\varepsilon}_{\hat{\bar{x}}}$. The boundedness of $\ddot{V}(\varepsilon_{\hat{\bar{x}}},\bar{x})$ implies the uniform continuity of $\dot{V}(\varepsilon_{\hat{\bar{x}}},\bar{x})$, which in turn implies that $\dot{V}(\varepsilon_{\hat{\bar{x}}},\bar{x})\to 0$ as $t\to\infty$ by applying Barbalat's Lemma. This implies $\bar{x}\to 0$ as $t\to\infty$,

which also means that $\bar{p} \to \bar{p}^{des}$ as $t \to \infty$. Hence, the target formation (1) is achieved while satisfying (8). ■

Remark 1: Note that conditions (23) and (24) are not part of the control laws. (24) is determined by the pair of matrices (L_e, D_L) that characterises the leader-follower graph topology. According to Theorem 1, we can first solve (24) to obtain the maximum value $\bar{\gamma}$ of γ that ensures $\Gamma \geq 0$. Then, the predefined largest decay rate l of performance functions $\rho_{\bar{x}_i}(t)$ cannot exceed this value $\bar{\gamma}$. Nevertheless, Theorem 1 can be useful in practical applications to predesign the maximum exponential decay rate of the performance functions.

Remark 2: Compared with existing work [11] that applies PPC for multi-agent systems, here we do not require that $D_L^T D_L$ to be positive definite in order to bound the quadratic term $-\varepsilon_{\hat{\bar{x}}}^T G_{\bar{x}} \mathcal{J}_{T_{\hat{\bar{x}}}} D_L^T D_L \mathcal{J}_{T_{\hat{\bar{x}}}} G_{\bar{x}} \varepsilon_{\hat{\bar{x}}}$ with the smallest eigenvalue of $D_L^T D_L$ because $D_L^T D_L > 0$ implies that the leader-follower multi-agent system can only have at most 1 follower. This would be very conservative, while Theorem 1 derives a more general result that allows for additional followers.

Remark 3: The complexity of the control synthesis is intuitively based on the number of leaders and the degree of the leaders (i.e., how many agents connect with the leaders). Since the method is decentralised, it is scalable in its implementation and can be applied to large scale leader-follower networks. Hence, if we judge the complexity by interaction between agents, it is indeed based on the leader-follower graph topology. Decentralization results in that the implementation is scalable with respect to the number of agents.

In the sequel, we will discuss the results for two specific classes of tree graphs, i.e., the chain and the star graph. First we consider the chain graph, which is widely used, for instance, in autonomous vehicle platooning.

Definition 1: A chain $\mathcal{G}^c = (\mathcal{V}^c, \mathcal{E}^c)$ is a tree graph with vertices set $\mathcal{V}^c = \{1, 2, \ldots, n\}, n \geq 2$ and edges set $\mathcal{E}^c = \{(i, i+1) \in \mathcal{V}^c \times \mathcal{V}^c \mid i \in \mathcal{V}^c \setminus \{n\}\}$ indexed by $e_i = (i, i+1), i = 1, 2, \ldots, n-1$.
Note that (23) in Theorem 1 is a sufficient but not necessary condition. For a chain graph, the matrix inequality (24) may be actually infeasible when the graph has 2 or more followers. The following result for $\mathcal{G}^c$ is derived.

Proposition 1: Consider the leader-follower multi-agent system Σ_1 described by (6) with the communication chain graph $\mathcal{G}^c = (\mathcal{V}^c, \mathcal{E}^c)$ and the followers set $\mathcal{V}_F^c = \{1, 2, \ldots, n_f\}$, the predefined performance functions $\rho_{\bar{x}_i}$ as in (10) and the transformed function $T_{\bar{x}_i}(\hat{\bar{x}}_i)$ as in (13) s.t. $T_{\bar{x}_i}(0) = 0$, and assume that the initial conditions $\bar{p}_i(0)$ are within the performance bounds (8). Then, the controlled system can achieve the target formation (1) and satisfy the prescribed performance bounds (8) when applying the control law (21) if and only if $n_f \leq 3$ holds. Specifically,

$$\begin{aligned} \max_{i=1,\ldots,m} (l_{\bar{x}_i}) = l \leq 2, \qquad n_f = 2; \\ \max_{i=1,\ldots,m} (l_{\bar{x}_i}) = l \leq 1, \qquad n_f = 3, \end{aligned} \tag{30}$$

are the respective conditions on the largest decay rate of the performance functions $\rho_{\bar{x}_i}$ such that the chain achieves the target formation (1) and satisfies (8) when applying (21).

Proof: The proof is based on showing that the evolution of the shifted relative position $\bar{x}_i(t)$ is always bounded by an exponential decay function $\rho_{\bar{x}_i}(t)$ for any $\bar{x}_i(0) \in (-\rho_{\bar{x}_i}(0), \rho_{\bar{x}_i}(0))$. For the if part, we consider the cases that $n_f \in \{0, 1, 2, 3\}$. When the chain graph has no follower or only one follower, that is $n_f = 0$ or $n_f = 1$, the result can be proved by using Theorem 1. Let $\bar{\gamma}$ be the maximum value of γ that ensures that (24) holds. By further choosing the decay rate of the performance functions (10) to satisfy (23), we can conclude that the controlled system achieves the target formation (1) within the prescribed performance bounds by applying (21) based on Theorem 1. When the chain has additional followers, the condition in Theorem 1 may be infeasible. But for this kind of special chain structure, we can resort to checking the edge dynamics (19) directly. It can be shown that $-L_e$ has elements given by $c_{ij} = -2$ when $i = j$, $c_{ij} = 1$ when $|i - j| = 1$ and $c_{ij} = 0$ otherwise in the case of a chain graph. We then rewrite (19) as

$$\left[\begin{array}{c} \dot{\bar{x}}_F \\ \hline \dot{\bar{x}}_L \end{array}\right] = \left[\begin{array}{c|c} \mathbf{A} & \mathbf{B} \\ \hline \mathbf{B}^T & \mathbf{C} \end{array}\right] \left[\begin{array}{c} \bar{x}_F \\ \hline \bar{x}_L \end{array}\right] + \left[\begin{array}{c} \mathbf{0} \\ \hline \mathbf{D} \end{array}\right] u, \tag{31}$$

where $\bar{x}_F \in \mathbb{R}^{(n_f - 1)}$ represents the edges between followers, while $\bar{x}_L \in \mathbb{R}^{n_l}$ represents the edge that connects the leader indexed by $n_f + 1$ and the follower indexed by n_f, and the edges between leaders. Both $\mathbf{A} \in \mathbb{R}^{(n_f-1)\times(n_f-1)}$, $\mathbf{C} \in \mathbb{R}^{n_l \times n_l}$ have the same structure as $-L_e$ but with different dimensions, i.e., both $\mathbf{A}$ and $\mathbf{C}$ have entries -2 in their principle diagonal and entries 1 in their subdiagonal and superdiagonal; $\mathbf{B}$ has an element 1 at row $(n_f - 1)$, column 1 (bottom left corner) that represents the connection between the follower node $\{n_f\}$ and the leader node $\{n_f + 1\}$. $\mathbf{0}$ is a $(n_f - 1) \times n_l$ zero matrix. $\mathbf{D} \in \mathbb{R}^{n_l \times n_l}$ has elements given by $\mathbf{d}_{ij} = 1$ when $i = j$, $\mathbf{d}_{ij} = -1$ when $i - j = 1$ and $\mathbf{d}_{ij} = 0$ otherwise. Then we can analyse the leader part $\bar{x}_L$ and the follower part $\bar{x}_F$ separately. For $\bar{x}_L$, it can be regarded as a chain graph with only one follower since $\bar{x}_L$ represents the edge that connects the leader indexed by $n_f + 1$ and the follower indexed by n_f, and the edges between leaders. By applying Theorem 1, we can prove that $\bar{x}_L$ reaches zero within the performance bounds (9) when applying the control law (21), which implies that the target formation can be achieved for the leader part while satisfying (8). We further rewrite the follower part as

$$\dot{\bar{x}}_F = \mathbf{A}\bar{x}_F + \mathbf{b}\bar{x}_\star, \tag{32}$$

where $\mathbf{b} \in \mathbb{R}^{(n_f-1)}$ is the first column of $\mathbf{B}$, i.e., with the last element equals to 1 and all other elements equal to 0; $\bar{x}_\star$ represents the edge between the follower node $\{n_f\}$ and the leader node $\{n_f + 1\}$. We can further rewrite the state evolution of (32) as $\bar{x}_F(t) = e^{\mathbf{A}t}\bar{x}_F(0) + \int_0^t e^{\mathbf{A}(t-\tau)}\mathbf{b}\bar{x}_\star(\tau)d\tau = M^T e^{\mathbf{\Lambda}t} M \bar{x}_F(0) + \int_0^t e^{\mathbf{A}(t-\tau)}\mathbf{b}\bar{x}_\star(\tau)d\tau = \bar{x}_F^0(t) + \int_0^t e^{\mathbf{A}(t-\tau)}\mathbf{b}\bar{x}_\star(\tau)d\tau$, where $\bar{x}_F^0(t) = \begin{bmatrix} \bar{x}_1^0(t) & \bar{x}_2^0(t) & \ldots & \bar{x}_{n_f-1}^0(t) \end{bmatrix}^T$ are the zero input trajectories, that is when $\bar{x}_\star(t) = 0, \forall t$; $\mathbf{A} = M^T \mathbf{\Lambda} M$, where $\mathbf{\Lambda}$ is a diagonal matrix with negative diagonal entries and equal to the eigenvalues of $\mathbf{A}$, which is due to $\mathbf{A}$ having the same structure as $-L_e$, and M is the matrix composed with the corresponding eigenvectors of $\mathbf{A}$. Without loss of generality, suppose all performance functions are the same and described by $\rho(t) = (\rho_0 - \rho_\infty)e^{-lt} + \rho_\infty$. When $n_f = 2$, $\bar{x}_F = \bar{x}_1$ and $\mathbf{A} = -2$, and we have that $\bar{x}_1^0(t) = M^T e^{\mathbf{\Lambda} t} M \bar{x}_1(0) = e^{-2t}\bar{x}_1(0) < \rho_0 e^{-2t}$. Then, $\bar{x}_1(t)$ is within the performance bound $\rho(t)$, i.e., $\bar{x}_1(t) < \rho(t), \forall t$, when $l \leq 2$ and in addition, $\int_0^t e^{-2(t-\tau)}\bar{x}_\star(\tau)d\tau < (\rho_0 - \bar{x}_1(0))e^{-2t} + \rho_\infty(1-e^{-2t})$, which can be ensured by tuning a large enough gain $g_{\bar{x}_2}$ for the edge e_2 that connects the follower indexed by 2 and the leader indexed by 3. When $n_f = 3$, we can derive a similar result. In particular, we now have that

$$\begin{bmatrix} \bar{x}_1^0(t) \\ \bar{x}_2^0(t) \end{bmatrix} = M^T e^{\mathbf{\Lambda} t} M \begin{bmatrix} \bar{x}_1(0) \\ \bar{x}_2(0) \end{bmatrix} < k \begin{bmatrix} \rho_0 \\ \rho_0 \end{bmatrix} e^{-t}, \tag{33}$$

with $k = 1$, which implies that $\bar{x}_i^0(t) < \rho_0 e^{-t}, i = \{1, 2\}$. Similarly, we can conclude that when $l \leq 1$, and in addition the tuning gain $g_{\bar{x}_3}$ for the edge e_3 that connects the follower indexed by 3 and the leader indexed by 4 is large enough, the controlled system achieves the target formation (1) within the prescribed performance bounds (8). Until now, we have proven the "if" part, the "only if" part can be proven through contradiction. Suppose that we have more than 3 followers and $n_f \geq 4$, we can then calculate the state evolution of the shifted relative position and it can be shown similarly that $\bar{x}_i^0(t) < k\rho_0 e^{\lambda_{\max}(\mathbf{A})t}, i = \{1, 2, \ldots, n_f - 1\}$, but with $k > 1$. This means that $\bar{x}_i^0(t)$ cannot be bounded by $\rho_0 e^{\lambda_{\max}(\mathbf{A})t}$ for any initial conditions within the performance bounds, i.e., for any $\bar{x}_i(0) \in (-\rho_{\bar{x}_i}(0), \rho_{\bar{x}_i}(0))$. Therefore, we can conclude that in order to achieve the target formation (1) within the performance bounds (8) for all initial conditions $\bar{p}_i(0)$ also within the performance bounds (8), n_f should be less or equal to 3. ■

Remark 4: Proposition 1 indicates that for a chain graph, in order to achieve the target formation (1) within the prescribed performance bounds (8), we can only have at most 3 consecutive followers at the end of the graph. In addition, when the initial relative position between 2 followers is close to the prescribed performance boundary (8), we need to tune a large enough gain for the edge that connects the follower indexed by n_f and the leader indexed by $n_f + 1$. Note that the statement "we can only have at most 3 consecutive followers at the end of the graph" relies on the specific structure of chain graphs or graphs that contain these chain graphs as subgraphs. The essential difference with a general leader-follower graph is that the chain graph that has consecutive followers contains fewer couplings between the leaders and followers.

Now we consider another specific class, in particular the star graph $\mathcal{G}^s = (\mathcal{V}^s, \mathcal{E}^s)$ which is defined as follows.

Definition 2: A star $\mathcal{G}^s = (\mathcal{V}^s, \mathcal{E}^s)$ is a tree graph with vertices set $\mathcal{V}^s = \{1, 2, \ldots, n\}, n \geq 2$ where vertex n is called the centering node, and the edges set $\mathcal{E}^s = \{(i, n) \in \mathcal{V}^s \times \mathcal{V}^s \mid i \in \mathcal{V}^s \setminus \{n\}\}$ indexed by $e_i = (i, n), i = 1, 2, \ldots, n-1$.

Then, the following result can be derived.

Proposition 2: Consider the leader-follower multi-agent system Σ_1 described by (6) with the communication star graph $\mathcal{G}^s = (\mathcal{V}^s, \mathcal{E}^s)$ and the leader set $\mathcal{V}_L^s = \{n\}$, the predefined performance functions $\rho_{\bar{x}_i}$ as in (10) and the transformed function $T_{\bar{x}_i}(\hat{\bar{x}}_i)$ as in (13) s.t. $T_{\bar{x}_i}(0) = 0$, and assume that the initial conditions $\bar{p}_i(0)$ are within the performance bounds (8). If

$$\max_{i=1,\ldots,m}(l_{\bar{x}_i}) = l \leq 1, \tag{34}$$

then the controlled system achieves the target formation (1) and satisfies the prescribed performance bounds (8) when applying the control law (21).

Proof: We can apply Theorem 1 to prove this Proposition for the specific case of star graphs. For a star graph defined as in Definition 2 with the centering node n as the only leader, the edge Laplacian L_e and matrices $D_L^T D_L, D_F^T D_F$ have special structures. $D_L^T D_L$ has all elements equal to 1, while $D_F^T D_F = L_e - D_L^T D_L$ is an identity matrix. L_e has the elements given by $c_{ij} = 2$ when $i = j$, and $c_{ij} = 1$ otherwise. Under this special structure of star graphs and according to Theorem 1, it can be verified that (23) is always feasible with $\bar{\gamma} = 1$, and from (34), we know that the condition $\bar{\gamma} \geq l = \max_{i=1,\ldots,m}(l_{\bar{x}_i})$ holds. Finally, by applying Theorem 1, for a star graph, when the performance functions (10) are chosen such that (34) holds, then we can conclude that the controlled system achieves the target formation (1) and satisfies the prescribed performance (8) when applying the control (21). ■

We conclude this subsection with the following observations. The results in this subsection indicate the trade-offs between the largest decay rate of the performance functions and the leader amount and positions. A sufficient condition for a general tree graph was derived in Theorem 1, under which the leader-follower multi-agent system (6) achieves the target formation (1) within the prescribed performance (8). It can be seen that (23) may be infeasible when the decay rate of the performance functions is too large. This means that we need to constrain the decay rate of the performance functions in order to achieve the target formation under prescribed performance guarantees within the leader-follower framework. This is reasonable since the followers only obey the first-order formation protocol without any additional external input. And the decay rate constraint differs for different graph topologies, leader amount and leader positions.

B. Formation control of second-order case using PPC

Similar to the first-order case, we first rewrite the dynamics of the second-order leader-follower multi-agent system (7) into the edge space in order to characterise the dynamics of the relative positions. Multiplying with D^T on both sides of (7) and using $\bar{x} = \bar{p} - \bar{p}^{des}$, we obtain the edge dynamics as

$$\Sigma_{e2} : \begin{bmatrix} \dot{\bar{x}} \\ \dot{\bar{v}} \end{bmatrix} = \begin{bmatrix} 0_m & I_m \\ -L_e & -L_e \end{bmatrix} \begin{bmatrix} \bar{x} \\ \bar{v} \end{bmatrix} + \begin{bmatrix} 0_{m \times n_l} \\ D_L^T \end{bmatrix} u. \tag{35}$$

For (35), we first design the reference velocity $v_d \in \mathbb{R}^n$ and the corresponding reference relative velocity $\bar{v}_d \in \mathbb{R}^m$ as:

$$v_d = -D\mathcal{J}_{T_{\hat{\bar{x}}}} G_{\bar{x}} \varepsilon_{\hat{\bar{x}}}; \qquad \bar{v}_d = -L_e \mathcal{J}_{T_{\hat{\bar{x}}}} G_{\bar{x}} \varepsilon_{\hat{\bar{x}}}, \tag{36}$$

where the parameters are the same as those defined in (21). We then define the relative velocity error vector as $\bar{e} = [\bar{e}_1, \ldots, \bar{e}_m]^T = \bar{v} - \bar{v}_d \in \mathbb{R}^m$. The insights here are basically resorting to first designing the reference relative velocity that can be proven to guarantee the prescribed performance for the relative positions. Then, by defining the relative velocity error vector, another PPC law with respect to the relative velocities is designed later to stabilise the relative velocity error vector also within certain prescribed performance bounds. Hence, we also define here the respective prescribed performance functions $\rho_{\bar{e}_i}(t)$, the transformed functions $T_{\bar{e}_i}(\hat{\bar{e}}_i)$ and the transformed error $\varepsilon_{\bar{e}_i}(\hat{\bar{e}}_i), i = 1, 2, \dots, m$ for the relative velocity errors. These terms are similar to those defined for the shifted relative positions. Note that enforcing the transformed errors $\varepsilon_{\bar{x}_i}(\hat{\bar{x}}_i), \varepsilon_{\bar{e}_i}(\hat{\bar{e}}_i)$ to be bounded will ensure the predefined prescribed performance guarantees. This can be achieved through the PPC laws that are going to be designed later.

The corresponding prescribed performance functions $\rho_{\bar{e}_i}(t)$ related to the relative velocity errors are defined as

$$\rho_{\bar{e}_i}(t) = (\rho_{\bar{e}_{i0}} - \rho_{\bar{e}_{i\infty}})e^{-l_{\bar{e}_i}t} + \rho_{\bar{e}_{i\infty}}, \tag{37}$$

and (37) is designed in a way such that the initial condition of $\bar{e}_i$ is within the performance bounds, i.e., $|\bar{e}_i(0)| < \rho_{\bar{e}_i}(0) = \rho_{\bar{e}_{i0}}, i = 1, 2, \dots, m$. The related prescribed performance region is described as

$$-\rho_{\bar{e}_i}(t) < \bar{e}_i(t) < \rho_{\bar{e}_i}(t). \tag{38}$$

Similar to (11), $\bar{e}_i(t)$ is normalized as

$$\hat{\bar{e}}_i(t) = \frac{\bar{e}_i(t)}{\rho_{\bar{e}_i}(t)}. \tag{39}$$

Then the normalized error is transformed through a transformed function $T_{\bar{e}_i}$ such that $T_{\bar{e}_i}(0) = 0$, with one example choice being

$$T_{\bar{e}_i}(\hat{\bar{e}}_i) = \ln\left(\frac{1 + \hat{\bar{e}}_i}{1 - \hat{\bar{e}}_i}\right). \tag{40}$$

Therefore, the transformed error $\varepsilon_{\bar{e}_i}$ is defined as

$$\varepsilon_{\bar{e}_i}(\hat{\bar{e}}_i) = T_{\bar{e}_i}(\hat{\bar{e}}_i). \tag{41}$$

Similar to (15), differentiating (41) with respect to time, we derive

$$\dot{\varepsilon}_{\bar{e}_i}(\hat{\bar{e}}_i) = \mathcal{J}_{T_{\bar{e}_i}}(\hat{\bar{e}}_i, t)[\dot{\bar{e}}_i + \alpha_{\bar{e}_i}(t)\bar{e}_i] \tag{42}$$

where

$$\mathcal{J}_{T_{\bar{e}_i}}(\hat{\bar{e}}_i, t) \triangleq \frac{\partial T_{\bar{e}_i}(\hat{\bar{e}}_i)}{\partial \hat{\bar{e}}_i}\frac{1}{\rho_{\bar{e}_i}(t)} > 0 \tag{43}$$

$$\alpha_{\bar{e}_i}(t) \triangleq -\frac{\dot{\rho}_{\bar{e}_i}(t)}{\rho_{\bar{e}_i}(t)} > 0 \tag{44}$$

are the normalized Jacobian of the transformation function $T_{\bar{e}_i}$ and the normalized derivative of the performance function, respectively. Using $T_{\bar{e}_i}(0) = 0$, we can derive that

$$\hat{\bar{e}}_i \frac{\partial \varepsilon_{\bar{e}_i}(\hat{\bar{e}}_i)}{\partial \hat{\bar{e}}_i}\varepsilon_{\bar{e}_i}(\hat{\bar{e}}_i) \geq \mu_{\bar{e}_i}\varepsilon^2_{\bar{e}_i}(\hat{\bar{e}}_i) \tag{45}$$

for some positive constant $\mu_{\bar{e}_i}$ [19]; (45) is useful for the forthcoming stability analysis.

For the leader-follower multi-agent system (35), the proposed controller applied to the leader agents is the composition of the term based on the prescribed performance of the relative velocity errors of the neighbouring agents:

$$u_j = -\sum_{i \in \Phi_j} g_{\bar{e}_i}\mathcal{J}_{T_{\bar{e}_i}}(\hat{\bar{e}}_i, t)\varepsilon_{\bar{e}_i}(\hat{\bar{e}}_i), \qquad j \in \mathcal{V}_L, \tag{46}$$

where $\Phi_j = \{i | (j, k) = i, k \in \mathcal{N}_j\}$, i.e., the set of all the edges that include agent $j \in \mathcal{V}_L$ as a node. Then the stack input vector is

$$u = -D_L \mathcal{J}_{T_{\hat{\bar{e}}}} G_{\bar{e}} \varepsilon_{\hat{\bar{e}}}, \tag{47}$$

where $\hat{\bar{e}} \in \mathbb{R}^m$ is the stack vector of transformed errors $\hat{\bar{e}}_i$, $G_{\bar{e}} \in \mathbb{R}^{m \times m}$ is a positive definite diagonal gain matrix with entries the positive constant parameters $g_{\bar{e}_i}$, $\mathcal{J}_{T_{\hat{\bar{e}}}} \triangleq \mathcal{J}_T(\hat{\bar{e}}, t) \in \mathbb{R}^{m \times m}$ is a time varying diagonal matrix with diagonal entries $\mathcal{J}_{T_{\bar{e}_i}}(\hat{\bar{e}}_i, t)$ given in (43), and $\varepsilon_{\hat{\bar{e}}} \triangleq \varepsilon(\hat{\bar{e}}) \in \mathbb{R}^m$ is the stack vector with entries $\varepsilon_{\bar{e}_i}(\hat{\bar{e}}_i)$.

Next, we derive the following result and will use Lyapunov-like methods to prove that the prescribed performance can be guaranteed for both relative positions and relative velocity errors. In addition, the target formation (1) can be achieved.

Theorem 2: Consider the leader-follower multi-agent system Σ_2 under Assumption 1 with dynamics (7), and the predefined performance functions $\rho_{\bar{x}_i}$ and $\rho_{\bar{e}_i}$ as in (10) and (37), respectively. The transformed functions $T_{\bar{x}_i}(\hat{\bar{x}}_i)$, $T_{\bar{e}_i}(\hat{\bar{e}}_i)$ are chosen as in (13), (40) respectively satisfying $T_{\bar{x}_i}(0) = 0, T_{\bar{e}_i}(0) = 0$, and assume that the initial conditions $\bar{x}_i(0)$ and $\bar{e}_i(0)$ are within the performance bounds (8) and (38), respectively. If the following condition holds:

$$\bar{\gamma} \geq l' = \max_{i=1,\dots,m}(l_{\bar{e}_i}), \tag{48}$$

where l' is the largest decay rate of $\rho_{\bar{e}_i}(t)$ and $\bar{\gamma}$ is the maximum value of γ that ensures:

$$\Gamma = \begin{bmatrix} D_L^T D_L & \frac{1}{2}\left(L_e - \gamma\left(I_m - D_L^T D_L\right)\right) \\ \frac{1}{2}\left(L_e - \gamma\left(I_m - D_L^T D_L\right)\right) & \gamma L_e \end{bmatrix} \geq 0, \tag{49}$$

then, the shifted relative position $\bar{x}$ under the control (47) converges to an arbitrary small ball around zero while satisfying (9). In addition, the relative velocity errors satisfy (38).

Proof: The proof is shown in the Appendix. ■

IV. SIMULATIONS

In this section, several simulation examples are presented in order to verify the results. The simulations' communication graphs are shown as Fig. 1, where the leaders and followers are represented by grey and white nodes, respectively. We choose, without loss of generality, the same $\rho_{\bar{x}_i}$ for all edges as $\rho_{\bar{x}_i}(t) = 4.9e^{-lt} + 0.1$. The decay rate l are different for the different simulation examples. For second-order leader-follower multi-agent systems, the prescribed performance functions $\rho_{\bar{e}_i}(t)$ related to the relative velocity errors are also chosen without loss of generality as the same, i.e., $\rho_{\bar{e}_i}(t) = 7e^{-l't} + 0.1$. For all $i = 1, \dots, m$, we choose $T_{\bar{x}_i}(\hat{\bar{x}}_i) = \ln\left(\frac{1+\hat{\bar{x}}_i}{1-\hat{\bar{x}}_i}\right); T_{\bar{e}_i}(\hat{\bar{e}}_i) = \ln\left(\frac{1+\hat{\bar{e}}_i}{1-\hat{\bar{e}}_i}\right)$. In addition, the prescribed performance bounds are depicted in black color in the following simulation plots.

In Fig. 1a, we first consider a tree graph with leaders set as $\mathcal{V}_L = \{4, 5, 6\}$. The positions of the agents are initialised as $p_1 = [1, 1]^T, p_2 = [2, 1]^T, p_3 = [1, 2]^T, p_4 = [2, 2]^T, p_5 = [3, 3]^T, p_6 = [4, 4]^T$ and the target relative position-based formation is $p^{des}_{41} = [-3, -3]^T, p^{des}_{42} = [-2, -3.5]^T, p^{des}_{43} = [-3, -3.5]^T, p^{des}_{54} = [-3.5, -3]^T, p^{des}_{65} = [-3.5, -3]^T$. According to Theorem 1, the matrix inequality is feasible with

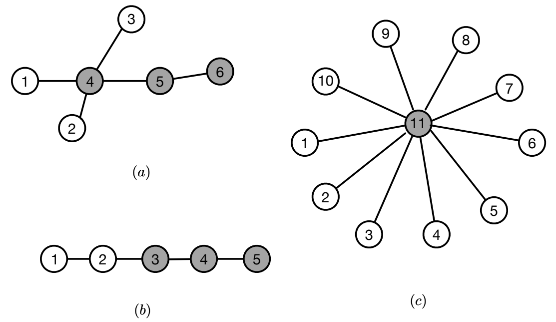

Fig. 1: Communication graphs with tree topologies.

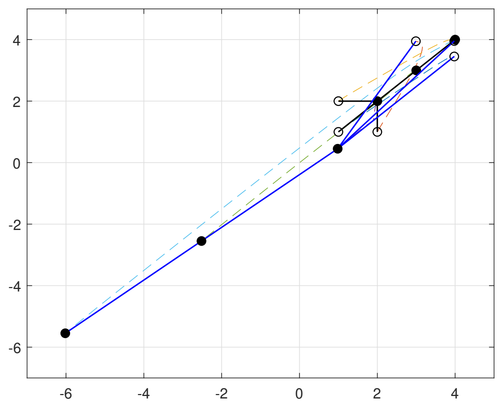

Fig. 2: Relative position-based formation control using PPC for the leader-follower multi-agent system under the graph as in Fig. 1a.

$\bar{\gamma} = 1$, hence it suffices that $l \leq \bar{\gamma} = 1$. The simulation result in two dimensions when applying the PPC law (21) with a gain matrix $G_{\bar{x}}$ whose diagonal entries are all equal to 1 is shown in Fig. 2. Here and also in the sequel, the dark lines show the initial formation, while the blue lines show the final positions of the agents. The dashed lines indicate the evolution of the agents. It can be seen that the target formation is achieved. In order to verify whether the prescribed performance is guaranteed, we only plot the evolution of the relative positions in y-direction between the neighboring agents due to space limitations, which are depicted in Fig. 4a. The red lines show the result without PPC, and we can see that the trajectories violate the prescribed performance bounds, which are improved by applying the PPC law (21). The result when applying PPC law is shown as the blue lines and we can observe that all the trajectories evolve within the prescribed performance bounds. Here the decay rate of the prescribed performance function is 1 and we can conclude that the controlled leader-follower multi-agent system achieves the target formation within the prescribed performance bound.

In Fig. 1b, we consider a chain graph with followers set as $\mathcal{V}_F = \{1, 2\}$ and $\mathcal{V}_F = \{1, 2, 3\}$. The relative positions are initialised as $\bar{p} = [4.8, 3, -2, 1]^T$ and the target relative position-based formation is $\bar{p}^{des} = 0_{5\times1}$. This means in this example, we consider a special class of formation, that is the consensus problem of leader-follower multi-agent systems

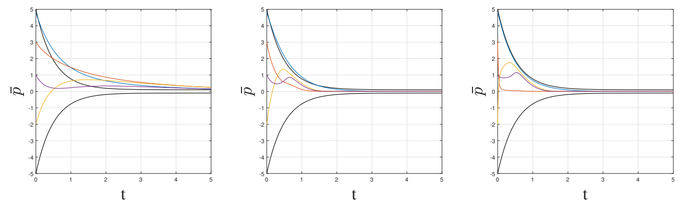

(a) Trajectories of the relative positions with $\mathcal{V}_F = \{1, 2\}$.

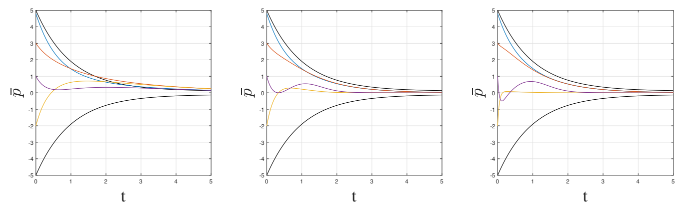

(b) Trajectories of the relative positions with $\mathcal{V}_F = \{1, 2, 3\}$.

Fig. 3: The left figures show the trajectories of relative positions without PPC, while the controlled systems with the PPC law but different gain matrix are shown in the middle and right figures, respectively under the graph as in Fig. 1b

in one dimension and we will only show the evolution of the trajectories in the edge space. When $\mathcal{V}_F = \{1, 2\}$, the simulation results are shown in Fig. 3a, where the left figure shows the simulation result without additional control. Here the decay rate of the prescribed performance function is 2. We can see that the trajectories violate the performance bound, which is improved as shown in the middle figure by applying the PPC law (21) with gain matrix $G_{\bar{x}} = diag(1, 10, 1, 1)$, where $diag(a_1, a_2, \ldots, a_n)$ represents the diagonal matrix with diagonal entries $a_1, a_2, \ldots, a_n$ and $g_{\bar{x}_2} = 10$ is tuned for leader $\{3\}$ that connects the followers. However, it can be seen that the trajectories still intersect the performance bound. We then increase $g_{\bar{x}_2}$ to 200, and the simulation result is shown in the right figure. We can see that the controlled system achieves consensus within the performance bound. When $\mathcal{V}_F = \{1, 2, 3\}$, the simulation results are shown as in Fig. 3b, in which the decay rate of the prescribed performance function is 1. Similarly, it can be seen in the left figure that the trajectories intersect the performance bound when there is no extra input, which is improved as shown in the middle and right figure by applying the PPC law (21) with gain matrix $G_{\bar{x}} = diag(1, 1, 10, 1)$ and $G_{\bar{x}} = diag(1, 1, 100, 1)$, respectively. We can also conclude that the controlled system achieves consensus within the performance bound.

In Fig. 1c, we consider a star graph with only one leader as $\mathcal{V}_L = \{11\}$, and all the agents are initialised at the origin. The target relative position-based formation is $\bar{p}_1^{des} = [-4, -4]^T, \bar{p}_2^{des} = [-3, 3]^T, \bar{p}_3^{des} = [2, -2]^T, \bar{p}_4^{des} = [3, 3]^T, \bar{p}_5^{des} = [-4.9, 0]^T, \bar{p}_6^{des} = [-1, -4.8]^T, \bar{p}_7^{des} = [-4.7, 4.5]^T, \bar{p}_8^{des} = [4, 1]^T, \bar{p}_9^{des} = [-1, 4.8]^T, \bar{p}_{10}^{des} = [-4.8, -2]^T$. According to Theorem 1, the matrix inequality is feasible with $\bar{\gamma} = 1$, hence it suffices that $l \leq \bar{\gamma} = 1$. The two dimension simulation result when applying the PPC law (21) with a gain matrix $G_{\bar{x}}$ whose diagonal entries are all equal to 1 is shown in Fig. 5. It can be shown that the leader-follower multi-agent system is initialised at the origin

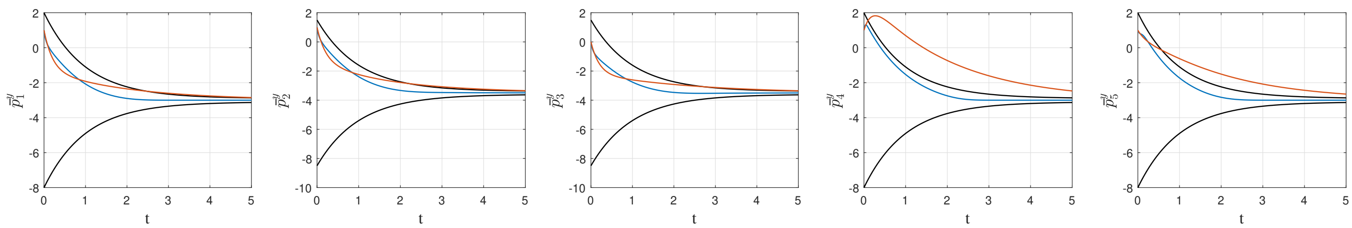

(a) Trajectories of the relative positions under the communication graph as in Fig. 1a.

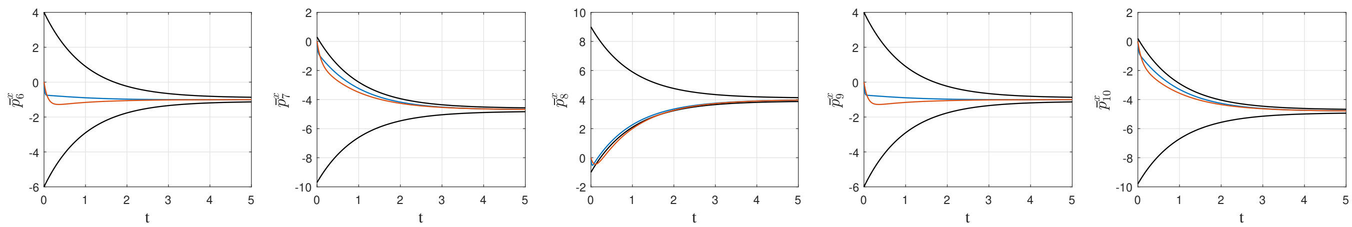

(b) Trajectories of the relative positions for the star graph as in Fig. 1c.

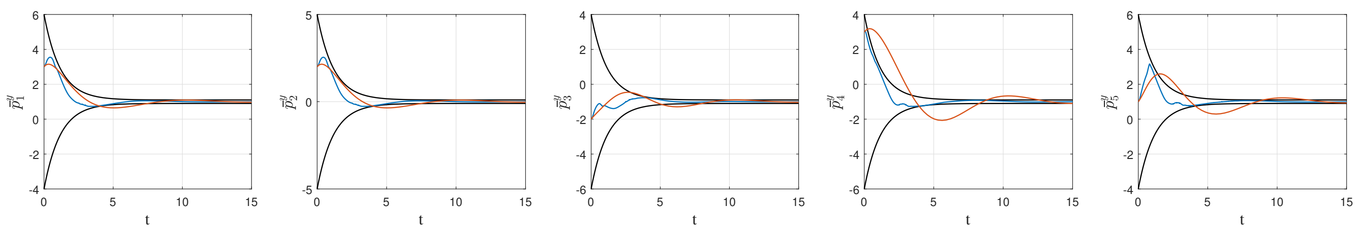

(c) Trajectories of the relative positions under the graph as in Fig. 1a for the second-order multi-agent system Σ_2 as in (7).

Fig. 4: Trajectories of the relative positions for different simulation examples. The blue and red lines indicate the results with and without PPC, respectively.

and the target formation is achieved as indicated by the blue lines. The evolution of the relative positions between the neighboring agents is depicted in Fig. 4b and here we only show the result for 5 edges in the x-direction due to space limitations. It is shown that the trajectories (red lines) intersect the performance bounds slightly when there is no extra input, which can be improved by applying the PPC law (21) such that the controlled system achieves the target formation within the performance bound as shown by the blue lines. Here the decay rate of the prescribed performance function is 1.

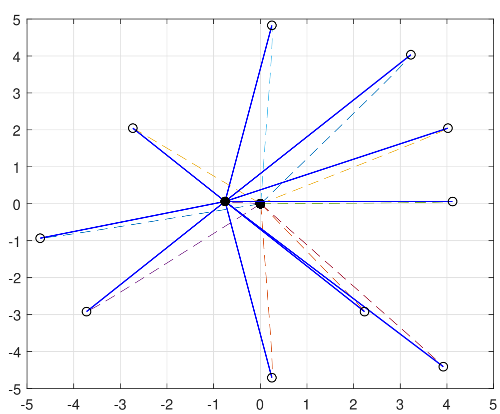

Fig. 5: Relative position-based formation control using PPC for the star graph as in Fig. 1c.

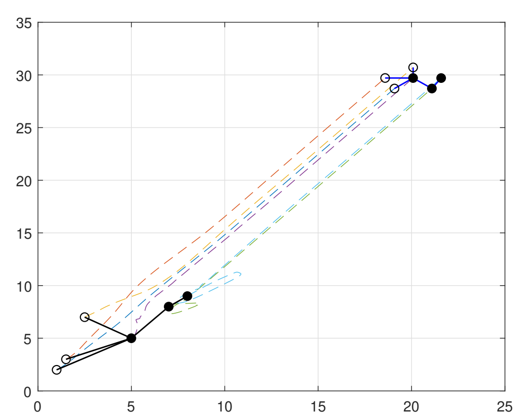

Fig. 6: Relative position-based formation control using PPC for the second-order leader-follower multi-agent system under the communication graph as in Fig. 1a.

Now we consider the topology as in Fig. 1a again for the case of a second-order leader-follower multi-agent system. The positions and velocities are initialised as $p_1 = [1,2]^T, p_2 = [1.5,3]^T, p_3 = [2.5,7]^T, p_4 = [5,5]^T, p_5 = [7,8]^T, p_6 = [8,9]^T$ and $v_1 = [1,1]^T, v_2 = [1,1]^T, v_3 = [1,1]^T, v_4 = [2,2]^T, v_5 = [3,3]^T, v_6 = [4,4]^T$, respectively. The target relative position-based formation is $p_{41}^{des} = [1,1]^T, p_{42}^{des} = [1.5,0]^T, p_{43}^{des} = [0,-1]^T, p_{54}^{des} = [1,-1]^T, p_{65}^{des} = [0.5,1]^T$. According to Theorem 2, the matrix inequality is feasible with

$\bar{\gamma}=1$, and l, l' chosen to be 0.85 and 0.9 respectively, and thus satisfying the constraint $l' \leq \bar{\gamma}=1$. The two dimensional simulation result when applying the PPC control law (47) with gain matrices $G_{\bar{x}}, G_{\bar{e}}$ whose diagonal entries are all equal to 1 is shown in Fig. 6. It can be seen that the target formation is achieved. Next, we plot the evolution of the relative positions between the neighboring agents in y-direction, which are depicted in Fig. 4c. The red lines show the result without PPC, and we can see that all the trajectories intersect the prescribed performance bounds, which are improved by applying the PPC law (47). Here the decay rate of the prescribed performance function is 0.85 and we can conclude that the controlled second order leader-follower multi-agent system achieves the target formation within the prescribed performance bounds.

V. CONCLUSIONS

In this paper, we have studied relative position-based formation control problems of leader-follower multi-agent systems with prescribed performance bounds for both first and second-order dynamics. For the first-order leader-follower multi-agent systems, under the assumption of tree graphs, a distributed prescribed performance control law has been proposed for the group of leaders in order to drive the followers such that the entire system can achieve the target formation under prescribed performance guarantees. We have proved that when the decay rate of the performance functions is within a sufficient bound, the target formation along with the performance guarantees can be obtained. In addition, the two specific classes of chain and star graphs that can have additional followers have been investigated. For the second-order leader-follower multi-agent systems, we have proved that when the decay rate of the performance functions of the relative velocity errors is within a sufficient bound, the relative velocity errors can also evolve within certain performance bounds.

Future research directions include considering more general graphs with circles, applying other transient approaches and also investigating leader selection problems.

APPENDIX

A. Proof of Theorem 2

Proof: The proof is based on the following three steps. We first show that there exists a maximal solution for both $\hat{\bar{x}}$ and $\hat{\bar{e}}$. Equivalently, that $\hat{\bar{x}}_i(t)$ and $\hat{\bar{e}}_i(t)$ remain in $\mathcal{D}_{\bar{x}_i}$ and $\mathcal{D}_{\bar{e}_i}=(-1,1)$, respectively within the maximal time solution interval $[0,\tau_{\max})$, where $\mathcal{D}_{\bar{x}_i}$ is defined in (12). Next, we prove that the proposed control strategy restricts $\hat{\bar{x}}_i(t)$ and $\hat{\bar{e}}_i(t)$ in compact subsets of $\mathcal{D}_{\bar{x}_i}$ and $\mathcal{D}_{\bar{e}_i}$ for $t\in[0,\tau_{\max})$, which by contradiction results in $\tau_{\max}=\infty$ in the last step and the proof is completed. In the sequel, we show the proof in detail step by step. We first define the target open set $\mathcal{D}=\mathcal{D}_{\bar{x}}\times\mathcal{D}_{\bar{e}}$ such that:

$$\begin{aligned}\mathcal{D}_{\bar{x}} &= \mathcal{D}_{\bar{x}_1}\times\mathcal{D}_{\bar{x}_2}\times\cdots\times\mathcal{D}_{\bar{x}_m},\\ \mathcal{D}_{\bar{e}} &= \mathcal{D}_{\bar{e}_1}\times\mathcal{D}_{\bar{e}_2}\times\cdots\times\mathcal{D}_{\bar{e}_m}.\end{aligned} \tag{50}$$

Step 1. Since the initial conditions $\bar{p}_i(0)$ are chosen within the performance bounds (8), this implies that the initial conditions $\bar{x}_i(0)$ are within the performance bounds (9). And since the initial conditions $\bar{e}_i(0)$ are chosen within the performance bounds (38), we can verify that the initial normalized shifted relative positions $\hat{\bar{x}}(0)$ and the initial normalized relative velocity errors $\hat{\bar{e}}(0)$ are within the open sets $\mathcal{D}_{\bar{x}}$ and $\mathcal{D}_{\bar{e}}$, respectively. We can conclude that $z(0)\in\mathcal{D}$, where $z(t)=[\hat{\bar{x}}(t),\hat{\bar{e}}(t)]^T$. By calculating the derivative of $\hat{\bar{x}}(t)$ and $\hat{\bar{e}}(t)$, we can verify that $\dot{z}$ is continuous and also locally Lipschitz on z. Hence, according to Theorem 54 of [20], there exists a maximal solution $z(t)$ in a time interval $[0,\tau_{\max})$ such that $z(t)\in\mathcal{D}, \forall t\in[0,\tau_{\max})$.

Step 2. Based on Step 1, we know that $\bar{x}_i$ and $\bar{e}_i$ satisfy (9) and (38), respectively for all $t\in[0,\tau_{\max})$. We first consider the Lyapunov-like function $V_{\bar{x}}=\frac{1}{2}\varepsilon_{\hat{\bar{x}}}^T G_{\bar{x}}\varepsilon_{\hat{\bar{x}}}$ related to the relative positions. Differentiating $V_{\bar{x}}$ with respect to time and using the stacked vector version of equation (15), we obtain

$$\dot{V}_{\bar{x}}=\varepsilon_{\hat{\bar{x}}}^T G_{\bar{x}}\dot{\varepsilon}_{\hat{\bar{x}}}=\varepsilon_{\hat{\bar{x}}}^T G_{\bar{x}}\mathcal{J}_{T_{\hat{\bar{x}}}}(\dot{\bar{x}}+\alpha_{\bar{x}}(t)\bar{x}), \tag{51}$$

where $\alpha_{\bar{x}}(t)$ is the diagonal matrix with diagonal entries $\alpha_{\bar{x}_i}(t)$ and we know that $\alpha_{\bar{x}_i}(t)<l_{\bar{x}_i}, \forall t$ according to (26). Since $\dot{\bar{x}}=\bar{v}=\bar{v}_d+\bar{e}$ where $\bar{v}_d$ is given in (36), we obtain $\dot{\bar{x}}=-L_e\mathcal{J}_{T_{\hat{\bar{x}}}}G_{\bar{x}}\varepsilon_{\hat{\bar{x}}}+\bar{e}$, and then by replacing $\dot{\bar{x}}$ in (51), we further derive that

$$\begin{aligned}\dot{V}_{\bar{x}} =&\varepsilon_{\hat{\bar{x}}}^T G_{\bar{x}}\mathcal{J}_{T_{\hat{\bar{x}}}}(-L_e\mathcal{J}_{T_{\hat{\bar{x}}}}G_{\bar{x}}\varepsilon_{\hat{\bar{x}}}+\bar{e}+\alpha_{\bar{x}}(t)\bar{x})\\ =&-\varepsilon_{\hat{\bar{x}}}^T G_{\bar{x}}\mathcal{J}_{T_{\hat{\bar{x}}}}L_e\mathcal{J}_{T_{\hat{\bar{x}}}}G_{\bar{x}}\varepsilon_{\hat{\bar{x}}}+\varepsilon_{\hat{\bar{x}}}^T G_{\bar{x}}\mathcal{J}_{T_{\hat{\bar{x}}}}\bar{e}\\ &+\varepsilon_{\hat{\bar{x}}}^T G_{\bar{x}}\mathcal{J}_{T_{\hat{\bar{x}}}}\alpha_{\bar{x}}(t)\bar{x}\\ \leq&-\lambda_{\min}(L_e)\|\varepsilon_{\hat{\bar{x}}}^T G_{\bar{x}}\mathcal{J}_{T_{\hat{\bar{x}}}}\|^2+\|\varepsilon_{\hat{\bar{x}}}^T G_{\bar{x}}\mathcal{J}_{T_{\hat{\bar{x}}}}\|\bar{M}_{\bar{x}},\end{aligned} \tag{52}$$

where $\bar{M}_{\bar{x}}$ is a positive constant satisfying

$$\|\bar{e}+\alpha_{\bar{x}}(t)\bar{x}\|\leq\bar{M}_{\bar{x}}. \tag{53}$$

(53) holds for a bounded $\bar{M}_{\bar{x}}$ due to the boundedness of $\alpha_{\bar{x}_i}(t)$ as shown in (26) and the boundedness of $\bar{x}_i, \bar{e}_i, i=1,\cdots,m$, for $t\in[0,\tau_{\max})$, which is shown in the beginning of Step 2. Then, we can conclude that $\dot{V}_{\bar{x}}<0$ when $\|\varepsilon_{\hat{\bar{x}}}^T G_{\bar{x}}\mathcal{J}_{T_{\hat{\bar{x}}}}\|>\frac{\bar{M}_{\bar{x}}}{\lambda_{\min}(L_e)}$. This condition is guaranteed when $\|\varepsilon_{\hat{\bar{x}}}\|>\frac{\bar{M}_{\bar{x}}}{\underline{\beta}\lambda_{\min}(L_e)}$ with $\underline{\beta}$ selected satisfying that $G_{\bar{x}}\mathcal{J}_{T_{\hat{\bar{x}}}}\geq\underline{\beta}I_m$. The reason is due to that $G_{\bar{x}}\mathcal{J}_{T_{\hat{\bar{x}}}}$ is a diagonal positive definite matrix, and we can thus derive the inequality $\|\varepsilon_{\hat{\bar{x}}}^T G_{\bar{x}}\mathcal{J}_{T_{\hat{\bar{x}}}}\|\geq\|\varepsilon_{\hat{\bar{x}}}^T\underline{\beta}I_m\|=\underline{\beta}\|\varepsilon_{\hat{\bar{x}}}\|$. Then, $\underline{\beta}\|\varepsilon_{\hat{\bar{x}}}\|>\frac{\bar{M}_{\bar{x}}}{\lambda_{\min}(L_e)}$, i.e., $\|\varepsilon_{\hat{\bar{x}}}\|>\frac{\bar{M}_{\bar{x}}}{\underline{\beta}\lambda_{\min}(L_e)}$ will ensure that $\|\varepsilon_{\hat{\bar{x}}}^T G_{\bar{x}}\mathcal{J}_{T_{\hat{\bar{x}}}}\|>\frac{\bar{M}_{\bar{x}}}{\lambda_{\min}(L_e)}$ holds. Hence, it can be concluded that $\|\varepsilon_{\hat{\bar{x}}}\|$ is upper bounded by

$$\|\varepsilon_{\hat{\bar{x}}}\|\leq\bar{\varepsilon}_1=\max\left\{\|\varepsilon_{\hat{\bar{x}}}(0)\|,\frac{\bar{M}_{\bar{x}}}{\underline{\beta}\lambda_{\min}(L_e)}\right\}, \tag{54}$$

$\forall t\in[0,\tau_{\max})$. Due to the boundedness of $\|\varepsilon_{\hat{\bar{x}}}\|$ in $t\in[0,\tau_{\max})$, we can restrict $\hat{\bar{x}}_i$ in a compact subset of $\mathcal{D}_{\bar{x}_i}$ as

$$\hat{\bar{x}}_i(t)\in[\underline{\delta}_{\bar{x}_i},\bar{\delta}_{\bar{x}_i}]\triangleq[-T_{\bar{x}_i}^{-1}(\bar{\varepsilon}_1),T_{\bar{x}_i}^{-1}(\bar{\varepsilon}_1)]\subset\mathcal{D}_{\bar{x}_i}, \tag{55}$$

where $T_{\bar{x}_i}^{-1}$ is the inverse function of the transformed function $T_{\bar{x}_i}$. $T_{\bar{x}_i}^{-1}$ always exists because $T_{\bar{x}_i}$ is a smooth and strictly increasing function. Therefore, the reference relative velocity vector $\bar{v}_d$ as designed in (36) and its derivative $\dot{\bar{v}}_d$ are both bounded in $t\in[0,\tau_{\max})$. Moreover, since $\bar{v}=\bar{v}_d+\bar{e}$, we can also conclude that $\bar{v}(t)$ is bounded for all $t\in[0,\tau_{\max})$ due to the boundedness of $\bar{v}_d$ and $\bar{e}$.

Next, for the velocity part, we consider the Lyapunov-like function $V_{\bar{e}} = \frac{1}{2}\varepsilon_{\hat{\bar{e}}}^T G_{\bar{e}} \varepsilon_{\hat{\bar{e}}} + \frac{\gamma}{2}\bar{e}^T\bar{e}$. Differentiating $V_{\bar{e}}$ with respect to time and using the stacked vector version of equation (42), we obtain

$$\begin{aligned} \dot{V}_{\bar{e}} &= \varepsilon_{\hat{\bar{e}}}^T G_{\bar{e}} \dot{\varepsilon}_{\hat{\bar{e}}} + \gamma \bar{e}^T \dot{\bar{e}} \\ &= \varepsilon_{\hat{\bar{e}}}^T G_{\bar{e}} \mathcal{J}_{T_{\hat{\bar{e}}}} (\dot{\bar{e}} + \alpha_{\bar{e}}(t)\bar{e}) + \gamma \bar{e}^T \dot{\bar{e}}. \end{aligned} \tag{56}$$

Then, from (35) we know that $\dot{\bar{v}} = -L_e\bar{x} - L_e\bar{v} + D_L^T u$. Since $\bar{v} = \bar{e} + \bar{v}_d$, and substituting the control strategy (47), we derive that $\dot{\bar{e}} = \dot{\bar{v}} - \dot{\bar{v}}_d = -L_e\bar{e} - L_e\bar{v}_d - L_e\bar{x} - D_L^T D_L \mathcal{J}_{T_{\hat{\bar{e}}}} G_{\bar{e}} \varepsilon_{\hat{\bar{e}}} - \dot{\bar{v}}_d$. Thus, replacing the above expression of $\dot{\bar{e}}$ in (56) and denoting $\Omega = -L_e\bar{v}_d - L_e\bar{x} - \dot{\bar{v}}_d$, we further obtain

$$\begin{aligned} \dot{V}_{\bar{e}} =& \varepsilon_{\hat{\bar{e}}}^T G_{\bar{e}} \mathcal{J}_{T_{\hat{\bar{e}}}} (-L_e\bar{e} - D_L^T D_L \mathcal{J}_{T_{\hat{\bar{e}}}} G_{\bar{e}} \varepsilon_{\hat{\bar{e}}} + \alpha_{\bar{e}}(t)\bar{e} + \Omega) \\ &+ \gamma \bar{e}^T (-L_e\bar{e} - D_L^T D_L \mathcal{J}_{T_{\hat{\bar{e}}}} G_{\bar{e}} \varepsilon_{\hat{\bar{e}}} + \Omega) \\ =& - \varepsilon_{\hat{\bar{e}}}^T G_{\bar{e}} \mathcal{J}_{T_{\hat{\bar{e}}}} D_L^T D_L \mathcal{J}_{T_{\hat{\bar{e}}}} G_{\bar{e}} \varepsilon_{\hat{\bar{e}}} - \varepsilon_{\hat{\bar{e}}}^T G_{\bar{e}} \mathcal{J}_{T_{\hat{\bar{e}}}} L_e \bar{e} \\ &+ \varepsilon_{\hat{\bar{e}}}^T G_{\bar{e}} \mathcal{J}_{T_{\hat{\bar{e}}}} \alpha_{\bar{e}}(t)\bar{e} - \gamma \varepsilon_{\hat{\bar{e}}}^T G_{\bar{e}} \mathcal{J}_{T_{\hat{\bar{e}}}} D_L^T D_L \bar{e} - \gamma \bar{e}^T L_e \bar{e} \\ &+ \varepsilon_{\hat{\bar{e}}}^T G_{\bar{e}} \mathcal{J}_{T_{\hat{\bar{e}}}} \Omega + \gamma \bar{e}^T \Omega, \end{aligned} \tag{57}$$

Adding and subtracting $\gamma \varepsilon_{\hat{\bar{e}}}^T G_{\bar{e}} \mathcal{J}_{T_{\hat{\bar{e}}}} \bar{e}$ on the right hand side of (57), we obtain

$$\begin{aligned} \dot{V}_{\bar{e}} =& - \varepsilon_{\hat{\bar{e}}}^T G_{\bar{e}} \mathcal{J}_{T_{\hat{\bar{e}}}} (\gamma I_m - \alpha_{\bar{e}}(t))\bar{e} \\ &- \varepsilon_{\hat{\bar{e}}}^T G_{\bar{e}} \mathcal{J}_{T_{\hat{\bar{e}}}} D_L^T D_L \mathcal{J}_{T_{\hat{\bar{e}}}} G_{\bar{e}} \varepsilon_{\hat{\bar{e}}} \\ &- \varepsilon_{\hat{\bar{e}}}^T G_{\bar{e}} \mathcal{J}_{T_{\hat{\bar{e}}}} L_e \bar{e} - \gamma \bar{e}^T L_e \bar{e} \\ &+ \gamma \varepsilon_{\hat{\bar{e}}}^T G_{\bar{e}} \mathcal{J}_{T_{\hat{\bar{e}}}} (I_m - D_L^T D_L)\bar{e} + \varepsilon_{\hat{\bar{e}}}^T G_{\bar{e}} \mathcal{J}_{T_{\hat{\bar{e}}}} \Omega + \gamma \bar{e}^T \Omega \\ =& - \varepsilon_{\hat{\bar{e}}}^T G_{\bar{e}} \mathcal{J}_{T_{\hat{\bar{e}}}} (\gamma I_m - \alpha_{\bar{e}}(t))\bar{e} + \varepsilon_{\hat{\bar{e}}}^T G_{\bar{e}} \mathcal{J}_{T_{\hat{\bar{e}}}} \Omega + \gamma \bar{e}^T \Omega \\ &- y^T \begin{bmatrix} D_L^T D_L & \frac{1}{2}\big(L_e - \gamma(I_m - D_L^T D_L)\big) \\ \frac{1}{2}\big(L_e - \gamma(I_m - D_L^T D_L)\big) & \gamma L_e \end{bmatrix} y \\ =& - \varepsilon_{\hat{\bar{e}}}^T G_{\bar{e}} \mathcal{J}_{T_{\hat{\bar{e}}}} (\gamma I_m - \alpha_{\bar{e}}(t))\bar{e} - y^T \Gamma y \\ &+ \varepsilon_{\hat{\bar{e}}}^T G_{\bar{e}} \mathcal{J}_{T_{\hat{\bar{e}}}} \Omega + \gamma \bar{e}^T \Omega \end{aligned} \tag{58}$$

with $y = \begin{bmatrix} \varepsilon_{\hat{\bar{e}}}^T G_{\bar{e}} \mathcal{J}_{T_{\hat{\bar{e}}}} & \bar{e}^T \end{bmatrix}^T$, and where the block matrix Γ is defined in (49). We have that $G_{\bar{e}} \mathcal{J}_{T_{\hat{\bar{e}}}}$ is a diagonal positive definite matrix. Using (26), we can verify that $(\gamma I_m - \alpha_{\bar{e}}(t))$ is a diagonal positive definite matrix if $\gamma \geq l' = \max(l_{\bar{e}_i}) > \bar{\alpha}' = \sup \alpha_{\bar{e}_i}(t)$. Since $T_{\bar{e}_i}$ is smooth, strictly increasing and $T_{\bar{e}_i}(0) = 0$, we have $\varepsilon_{\bar{e}_i}(\hat{\bar{e}}_i)\hat{\bar{e}}_i \geq 0$. Then, by setting $\gamma := \theta + \bar{\alpha}'$, with θ being a positive constant, we get $-\varepsilon_{\hat{\bar{e}}}^T G_{\bar{e}} \mathcal{J}_{T_{\hat{\bar{e}}}} (\gamma I_m - \alpha_{\bar{e}}(t))\bar{e} \leq -\theta \varepsilon_{\hat{\bar{e}}}^T G_{\bar{e}} \mathcal{J}_{T_{\hat{\bar{e}}}} \bar{e}$ Then, according to (39), (43), we further obtain

$$-\theta \varepsilon_{\hat{\bar{e}}}^T G_{\bar{e}} \mathcal{J}_{T_{\hat{\bar{e}}}} \bar{e} = -\theta \varepsilon_{\hat{\bar{e}}}^T G_{\bar{e}} \frac{\partial \varepsilon_{\hat{\bar{e}}}}{\partial \hat{\bar{e}}} \hat{\bar{e}} \leq 0. \tag{59}$$

(59) holds because the transformed function $T_{\bar{e}_i}$ is smooth and strictly increasing and $\varepsilon_{\bar{e}_i}(\hat{\bar{e}}_i)\hat{\bar{e}}_i \geq 0$. Then, based on condition (48), and choosing $\gamma = \bar{\gamma}$, we obtain $-\varepsilon_{\hat{\bar{e}}}^T G_{\bar{e}} \mathcal{J}_{T_{\hat{\bar{e}}}} (\gamma I_m - \alpha_{\bar{e}}(t))\bar{e} \leq 0$ and $\Gamma \geq 0$. Then $\dot{V}_{\bar{e}}$ is upper bounded as

$$\dot{V}_{\bar{e}} \leq -\theta \varepsilon_{\hat{\bar{e}}}^T G_{\bar{e}} \frac{\partial \varepsilon_{\hat{\bar{e}}}}{\partial \hat{\bar{e}}} \hat{\bar{e}} + \varepsilon_{\hat{\bar{e}}}^T G_{\bar{e}} \mathcal{J}_{T_{\hat{\bar{e}}}} \Omega + \gamma \bar{e}^T \Omega, \tag{60}$$

Since $\bar{e}_i = \rho_{\bar{e}_i}\hat{\bar{e}}_i$ and $\hat{\bar{e}}_i$ can be mapped to $\varepsilon_{\bar{e}_i}(\hat{\bar{e}}_i)$ through the transformed function $T_{\bar{e}_i}(\hat{\bar{e}}_i)$, we can then define a mapping matrix Q between $\bar{e}$ and $\varepsilon_{\hat{\bar{e}}}$ in order to reorganise (60), i.e., $\bar{e} = Q\varepsilon_{\hat{\bar{e}}}$, where Q is a time-varying diagonal positive definite mapping matrix. This matrix Q always exists with the diagonal entries $q_i = \rho_{\bar{e}_i}\hat{\bar{e}}_i / \varepsilon_{\bar{e}_i}(\hat{\bar{e}}_i) > 0$. Then, (60) is rewritten as $\dot{V}_{\bar{e}} \leq -\theta \varepsilon_{\hat{\bar{e}}}^T G_{\bar{e}} \frac{\partial \varepsilon_{\hat{\bar{e}}}}{\partial \hat{\bar{e}}} \hat{\bar{e}} + \varepsilon_{\hat{\bar{e}}}^T (G_{\bar{e}} \mathcal{J}_{T_{\hat{\bar{e}}}} \Omega + \gamma Q \Omega)$. Next, according to inequality (45), we further derive that $\dot{V}_{\bar{e}} \leq -\theta\mu\|\varepsilon_{\hat{\bar{e}}}\|^2 + \|\varepsilon_{\hat{\bar{e}}}\|\bar{M}_{\bar{e}}$, where $\mu = \min(\mu_{\bar{e}_i}), i = 1, \cdots, m$ and $\mu_{\bar{e}_i}$ is defined in (45). $\bar{M}_{\bar{e}}$ is a positive constant satisfying

$$\|G_{\bar{e}} \mathcal{J}_{T_{\hat{\bar{e}}}} \Omega + \gamma Q \Omega\| \leq \bar{M}_{\bar{e}}. \tag{61}$$

(61) holds with a bounded $\bar{M}_{\bar{e}}$ due to the boundedness of $\bar{x}, \bar{v}_d, \dot{\bar{v}}_d$, $\forall t \in [0, \tau_{\max})$ as discussed in the relative position part. Similarly, it can be concluded that $\dot{V}_{\bar{e}} < 0$ when $\|\varepsilon_{\hat{\bar{e}}}\| > \frac{\bar{M}_{\bar{e}}}{\theta\mu}$ and further $\|\varepsilon_{\hat{\bar{e}}}\|$ is upper bounded by

$$\|\varepsilon_{\hat{\bar{e}}}\| \leq \bar{\varepsilon}_2 = \max\left\{\|\varepsilon_{\hat{\bar{e}}}(0)\|, \frac{\bar{M}_{\bar{e}}}{\theta\mu}\right\}, \tag{62}$$

$\forall t \in [0, \tau_{\max})$. Due to the boundedness of $\|\varepsilon_{\hat{\bar{e}}}\|$ in $t \in [0, \tau_{\max})$, we can restrict $\hat{\bar{e}}_i$ in a compact subset of $\mathcal{D}_{\bar{e}_i}$ as

$$\hat{\bar{e}}_i(t) \in [\underline{\delta}_{\bar{e}_i}, \bar{\delta}_{\bar{e}_i}] \triangleq [-T_{\bar{e}_i}^{-1}(\bar{\varepsilon}_2), T_{\bar{e}_i}^{-1}(\bar{\varepsilon}_2)] \subset \mathcal{D}_{\bar{e}_i}, \tag{63}$$

where $T_{\bar{e}_i}^{-1}$ is the inverse function of $T_{\bar{e}_i}$.

Step 3. Finally, we need to prove that $\tau_{\max}$ can be extended to ∞. According to (55) and (63), we know that $z(t) \in \mathcal{D}' = \mathcal{D}'_{\bar{x}} \times \mathcal{D}'_{\bar{e}}, \forall t \in [0, \tau_{\max})$, where $\mathcal{D}'_{\bar{x}} = [\underline{\delta}_{\bar{x}_1}, \bar{\delta}_{\bar{x}_1}] \times \cdots \times [\underline{\delta}_{\bar{x}_m}, \bar{\delta}_{\bar{x}_m}]$ and $\mathcal{D}'_{\bar{e}} = [\underline{\delta}_{\bar{e}_1}, \bar{\delta}_{\bar{e}_1}] \times \cdots \times [\underline{\delta}_{\bar{e}_m}, \bar{\delta}_{\bar{e}_m}]$. Hence, $\mathcal{D}' \subset \mathcal{D}$ is a nonempty and compact subset of $\mathcal{D}$ and it can be concluded that $z(t) \in \mathcal{D}', \forall t \in [0, \tau_{\max})$. Let us now assume that $\tau_{\max} < \infty$. According to Proposition C.3.6 of [20], there exists a $t' \in [0, \tau_{\max})$ such that $z(t') \notin \mathcal{D}'$, which leads to a contradiction. Hence, we conclude that $\tau_{\max}$ is extended to ∞, that is $z(t) \in \mathcal{D}' \subset \mathcal{D}, \forall t \geq 0$. Therefore $\varepsilon_{\hat{\bar{x}}}, \varepsilon_{\hat{\bar{e}}}$ are bounded for all $t \geq 0$ and the boundedness of the transformed errors $\varepsilon_{\hat{\bar{x}}}, \varepsilon_{\hat{\bar{e}}}$ implies that the shifted relative position $\bar{x}(t)$ and the relative velocity error $\bar{e}(t)$ evolve while satisfying (8) and (38), respectively for all $t \geq 0$. Finally, the convergence result is discussed. By choosing small enough $\rho_{\bar{x}_{i\infty}}$, we can conclude that $\bar{x}(t)$ achieves practical convergence in the sense that $\bar{x}_i \in (-\epsilon, \epsilon)$ as $t \to \infty$, where ϵ is close to 0 and satisfies $\epsilon \leq \rho_{\bar{x}_{i\infty}}, i = 1, \ldots, m$. The convergence of $\bar{x}(t)$ also implies that the target formation (1) is achieved. ■

Remark 5: The convergence result of $\bar{x}(t)$ in Theorem 2 is practical convergence since ϵ can be arbitrarily small but not exactly zero. This kind of practical convergence is also shown in [21], and is reasonable in practical design. Note that it cannot be guaranteed that the errors converge to zero.

References

[1] T. Balch and R. C. Arkin, "Behavior-based formation control for multirobot teams," *IEEE transactions on robotics and automation*, vol. 14, no. 6, pp. 926–939, 1998.

[2] K.-K. Oh, M.-C. Park, and H.-S. Ahn, "A survey of multi-agent formation control," *Automatica*, vol. 53, pp. 424–440, 2015.

[3] R. Olfati-Saber and R. M. Murray, "Consensus problems in networks of agents with switching topology and time-delays," *IEEE Transactions on automatic control*, vol. 49, no. 9, pp. 1520–1533, 2004.

[4] W. Ren and E. Atkins, "Distributed multi-vehicle coordinated control via local information exchange," *International Journal of Robust and Nonlinear Control: IFAC-Affiliated Journal*, vol. 17, no. 10-11, pp. 1002–1033, 2007.

[5] H. G. Tanner, "On the controllability of nearest neighbor interconnections," in *Decision and Control, 2004. CDC. 43rd IEEE Conference on*, vol. 3. IEEE, 2004, pp. 2467–2472.

[6] A. Y. Yazicioğlu and M. Egerstedt, "Leader selection and network assembly for controllability of leader-follower networks," in *American Control Conference (ACC), 2013*. IEEE, 2013, pp. 3802–3807.

[7] K. Fitch and N. E. Leonard, "Optimal leader selection for controllability and robustness in multi-agent networks," in *2016 European Control Conference (ECC)*. IEEE, 2016, pp. 1550–1555.

[8] S. Patterson and B. Bamieh, "Leader selection for optimal network coherence," in *49th IEEE Conference on Decision and Control (CDC)*. IEEE, 2010, pp. 2692–2697.

[9] C. P. Bechlioulis and G. A. Rovithakis, "Robust adaptive control of feedback linearizable mimo nonlinear systems with prescribed performance," *IEEE Transactions on Automatic Control*, vol. 53, no. 9, pp. 2090–2099, 2008.

[10] L. Macellari, Y. Karayiannidis, and D. V. Dimarogonas, "Multi-agent second order average consensus with prescribed transient behavior," *IEEE Transactions on Automatic Control*, vol. 62, no. 10, pp. 5282–5288, 2017.

[11] Y. Karayiannidis, D. V. Dimarogonas, and D. Kragic, "Multi-agent average consensus control with prescribed performance guarantees," in *Decision and Control (CDC), 2012 IEEE 51st Annual Conference on*. IEEE, 2012, pp. 2219–2225.

[12] A. Ilchmann, E. P. Ryan, and S. Trenn, "Tracking control: Performance funnels and prescribed transient behaviour," *Systems & Control Letters*, vol. 54, no. 7, pp. 655–670, 2005.

[13] I. Katsoukis and G. A. Rovithakis, "Output feedback leader-follower with prescribed performance guarantees for a class of unknown nonlinear multi-agent systems," in *2016 24th Mediterranean Conference on Control and Automation (MED)*. IEEE, 2016, pp. 1077–1082.

[14] F. Chen and D. V. Dimarogonas, "Consensus control for leader-follower multi-agent systems under prescribed performance guarantees," in *58th IEEE Conference on Decision and Control*. IEEE, 2019.

[15] ——, "Second order consensus for leader-follower multi-agent systems with prescribed performance," *IFAC-PapersOnLine*, vol. 52, no. 20, pp. 103–108, 2019.

[16] M. Mesbahi and M. Egerstedt, *Graph theoretic methods in multiagent networks*. Princeton University Press, 2010, vol. 33.

[17] D. Zelazo and M. Mesbahi, "Edge agreement: Graph-theoretic performance bounds and passivity analysis," *IEEE Transactions on Automatic Control*, vol. 56, no. 3, pp. 544–555, 2011.

[18] D. V. Dimarogonas and K. H. Johansson, "Stability analysis for multi-agent systems using the incidence matrix: quantized communication and formation control," *Automatica*, vol. 46, no. 4, pp. 695–700, 2010.

[19] Y. Karayiannidis and Z. Doulgeri, "Model-free robot joint position regulation and tracking with prescribed performance guarantees," *Robotics and Autonomous Systems*, vol. 60, no. 2, pp. 214–226, 2012.

[20] E. D. Sontag, *Mathematical control theory: deterministic finite dimensional systems*. Springer Science & Business Media, 2013, vol. 6.

[21] C. P. Bechlioulis and G. A. Rovithakis, "A low-complexity global approximation-free control scheme with prescribed performance for unknown pure feedback systems," *Automatica*, vol. 50, no. 4, pp. 1217–1226, 2014.

Fei Chen is currently a Ph.D. student in the Division of Decision and Control Systems at KTH Royal Institute of Technology (Sweden). He received his M.Sc. degree from the Systems and Control group in the Electrical Engineering Department at Eindhoven University of Technology (Netherlands) in 2016. He received his B.Sc. degree in the Department of Control Science and Engineering at Zhejiang University (China) in 2014. His research interests are situated on the edge between control theory and formal methods in computer science, with particular interests in formal verification and control synthesis for multi-agent systems under temporal logic specifications.

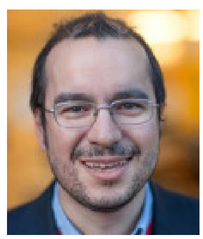

Dimos V. Dimarogonas was born in Athens, Greece, in 1978. He received the Diploma in Electrical and Computer Engineering in 2001 and the Ph.D. in Mechanical Engineering in 2007, both from the National Technical University of Athens (NTUA), Greece. Between May 2007 and March 2010, he held postdoctoral positions at KTH Royal Institute of Technology, Stockholm, Sweden and at LIDS, MIT, Boston, USA. He is currently a Professor at the Division of Decision and Control Systems, School of EECS, at the KTH Royal Institute of Technology. His current research interests include Multi-Agent Systems, Hybrid Systems and Control, Robot Navigation and Networked Control. He serves in the Editorial Board of Automatica and the IEEE Transactions on Control of Network Systems and is a Senior Member of the IEEE. He received an ERC Starting Grant in 2014, an ERC Consolidator Grant in 2019, and was awarded a Wallenberg Academy Fellow grant in 2015.